Fraunhofer
ITWM

M. Speckert, N. Ruf, K. Dreßler

Undesired drift of multibody models excited by measured accelerations or forces

Berichte des Fraunhofer ITWM, Nr. 162 (2009)

ISSN 1434-9973

Bericht 162 (2009)

Die Veröffentlichungen in der Berichtsreihe des Fraunhofer ITWM können bezogen werden über:

Fraunhofer-Institut für Techno- und
Wirtschaftsmathematik ITWM
Fraunhofer-Platz 1

67663 Kaiserslautern
Germany

Telefon: 06 31/3 16 00-0
Telefax: 06 31/3 16 00-10 99
E-Mail: info@itwm.fraunhofer.de
Internet: www.itwm.fraunhofer.de

Vorwort

Das Tätigkeitsfeld des Fraunhofer-Instituts für Techno- und Wirtschaftsmathematik ITWM umfasst anwendungsnahe Grundlagenforschung, angewandte Forschung sowie Beratung und kundenspezifische Lösungen auf allen Gebieten, die für Techno- und Wirtschaftsmathematik bedeutsam sind.

In der Reihe »Berichte des Fraunhofer ITWM« soll die Arbeit des Instituts kontinuierlich einer interessierten Öffentlichkeit in Industrie, Wirtschaft und Wissenschaft vorgestellt werden. Durch die enge Verzahnung mit dem Fachbereich Mathematik der Universität Kaiserslautern sowie durch zahlreiche Kooperationen mit internationalen Institutionen und Hochschulen in den Bereichen Ausbildung und Forschung ist ein großes Potenzial für Forschungsberichte vorhanden. In die Berichtreihe sollen sowohl hervorragende Diplom- und Projektarbeiten und Dissertationen als auch Forschungsberichte der Institutsmitarbeiter und Institutsgäste zu aktuellen Fragen der Techno- und Wirtschaftsmathematik aufgenommen werden.

Darüber hinaus bietet die Reihe ein Forum für die Berichterstattung über die zahlreichen Kooperationsprojekte des Instituts mit Partnern aus Industrie und Wirtschaft.

Berichterstattung heißt hier Dokumentation des Transfers aktueller Ergebnisse aus mathematischer Forschungs- und Entwicklungsarbeit in industrielle Anwendungen und Softwareprodukte – und umgekehrt, denn Probleme der Praxis generieren neue interessante mathematische Fragestellungen.

Prof. Dr. Dieter Prätzel-Wolters
Institutsleiter

Kaiserslautern, im Juni 2001

MULTIBODY DYNAMICS 2009, ECCOMAS Thematic Conference
K. Arczewski, J. Frączek, M. Wojtyra (eds.)
Warsaw, Poland, 29 June–2 July 2009

UNDESIRED DRIFT OF MULTIBODY MODELS EXCITED BY MEASURED ACCELERATIONS OR FORCES

Michael Speckert, Nikolaus Ruf, and Klaus Dressler

Department of Mathematical Methods in Dynamics and Durability
Fraunhofer Institute for Industrial and Financial Mathematics (ITWM)
Fraunhofer-Platz 1, 67663 Kaiserslautern, Germany
e-mails: Michael.Speckert@itwm.fraunhofer.de
Nikolaus.Ruf@itwm.fraunhofer.de
Klaus.Dressler@itwm.fraunhofer.de
web page: http://www.itwm.fhg.de/en/mdf/indexmdf/

Keywords: Multibody simulation, full vehicle model, force-based simulation, drift due to noise

Abstract. *In the ground vehicle industry it is often an important task to simulate full vehicle models based on the wheel forces and moments, which have been measured during driving over certain roads with a prototype vehicle. The models are described by a system of differential algebraic equations (DAE) or ordinary differential equations (ODE). The goal of the simulation is to derive section forces at certain components for a durability assessment. In contrast to handling simulations, which are performed including more or less complex tyre models, a driver model, and a digital road profile, the models we use here usually do not contain the tyres or a driver model. Instead, the measured wheel forces are used for excitation of the unconstrained model. This can be difficult due to noise in the input data, which leads to an undesired drift of the vehicle model in the simulation.*

This paper shortly describes the source of this effect by the theory of stochastic differential equations and explains, that this problem cannot be fully solved by a specialised numerical treatment of the underlying equations due to missing knowledge about the true trajectory of the vehicle. Several ways to deal with the problem are briefly reported. Among these, an algorithm for the calculation of the vehicles trajectory and orientation from additionally measured accelerations is described. However, here we also have to deal with the drift induced by the integration procedure and thus the usage of additional measurements on the velocity or position level (angular velocities or angles (orientation) of the vehicle body) is motivated.

Finally the theoretical considerations are exemplified using a vehicle model, which is simple enough for a rigorous treatment of the equations of motion and at the same time rich enough to show all the effects described before.

1 INTRODUCTION

In the ground vehicle industry, measurements on vehicles driving over test tracks or public roads are performed in order to derive loads for test rig or numerical verification. Often 100-200 different quantities at different spots of the vehicle are measured, among which we have wheel forces (measured at the hub), spring displacements, strains, or accelerations. The data can be used either for directly setting up rig tests for certain components (for example a test of a subframe based on measured strains) or for the excitation of multibody models of the vehicle in order to calculate section forces.

Besides the 'internal' excitation of the vehicle by steering, acceleration, or braking, the main 'external' excitation is given by the forces at the contact patches between tyres and ground. These are reaction forces, which in principle can be computed based on a digitised road profile, a tyre model as a part of the vehicle model, and a driver model driving the vehicle. However, this approach requires accurate tyre models as well as the digitised road. An alternative way of exciting the full vehicle model is to virtually cut off the tyres and use measured wheel forces as input. In the latter case, the interaction between the mechanism and the environment is via the section forces only.

While simulating such an unconstrained system based on section forces is very important in practice, it can be difficult due to noise in the input data. This leads to an undesired drift of the vehicle, which can be explained by the theory of stochastic differential equations. To circumvent such problems additional measurements are needed. Typically, measured accelerations of the vehicle body exist, but these alone do not help. Instead, data on the velocity or even displacement level are needed to deal with the drift.

In Sec. 2 the drift due to noisy input data during integration is studied using the most basic example of a point mass subject to a force. In Sec. 3 some investigations on how to circumvent the drift are reported. Finally in Sec. 4 we use a model of a simple demonstration vehicle to exemplify the theoretical considerations.

2 INTEGRATION OF NOISY DATA

In this section, we study a simple differential equation to illustrate the problems inherent in integrating noisy data. We make use of some basic results from stochastic analysis but do not treat them in great detail, as this is not the main focus of this paper. A brief introduction to the theory of stochastic differential equations (SDEs) with applications can be found in [8].

As an example, we consider the one-dimensional equation of motion for a point mass:

$$dx = v\,dt \quad , \quad dv = \left(\tfrac{f}{m} - \eta v\right) dt \quad , \quad x(0) = v(0) = 0 \tag{1}$$

This ODE describes the velocity $v(t)$ and position $x(t)$ of an object with mass $m > 0$ subject to the accelerating force $f(t)$, provided the object was at rest at time $t = 0$. A damping term (friction) proportional to the velocity is also included, with damping constant $\eta \geq 0$.

The problem now is to reconstruct the velocity and position based on measurements distorted by unsystematic errors, which we model as independent Gaussian random variables. If we denote the time step between observations by Δt, the forces we actually observe are

$$\tilde{f}(n\Delta t) \sim \mathrm{N}(f(n\Delta t), \sigma_M^2) \tag{2}$$

with some variance $\sigma_M^2 > 0$ representing the accuracy of the measurement device. The impact of the noise on the reconstructed velocity and position depends on the discretisation scheme we

choose to solve (1). We use the explicit Euler scheme for our example, as it permits us to study error propagation in terms of a simple SDE. To derive it, we begin with the difference equation for the velocity, taking the time step to be equal to the rate of observations:

$$\tilde{v}_{n+1} := \tilde{v}((n+1)\Delta t) := \tilde{v}_n + \left(\tfrac{f(n\Delta t)+\epsilon_n}{m} - \eta\tilde{v}_n\right)\Delta t \quad , \quad \tilde{v}_0 := \tilde{v}(0) := 0 \tag{3}$$

The errors ϵ_n are i.i.d. Gaussian random variables with mean zero and variance σ_M^2. If the true force is L^2-integrable and Δt sufficiently small, a solution of the difference equation approximates a solution of the following Itô-SDE on the discrete time grid given by Δt:

$$d\tilde{x} = \tilde{v}\,dt \quad , \quad d\tilde{v} = \left(\tfrac{f}{m} - \eta\tilde{v}\right)dt + \tfrac{\sigma}{m}dW(t) \quad , \quad \tilde{x}(0) = \tilde{v}(0) = 0 \tag{4}$$

To determine the variance σ^2 of the Brownian motion in the limiting case, we note that the variance of the increments is

$$\mathrm{Var}(\epsilon_n\Delta t) = \sigma_M^2(\Delta t)^2 \stackrel{!}{=} \sigma^2\Delta t \iff \sigma^2 = \sigma_M^2\Delta t \tag{5}$$

We have seen that if we solve the ODE (1) with perturbed forces using the explicit Euler scheme, what we actually do is construct a path of the solution of the SDE (4). Its usefulness for the purpose of simulation depends on how far it deviates from the actual values. As the individual errors have bounded variance, we might hope that $\tilde{v}$ and $\tilde{x}$ share this property. Unfortunately, this is only true for the velocity, and only if the damping constant η is positive:

The unique solution of (1) is

$$x(t) = \textstyle\int_0^t v(s)\,ds \quad , \quad v(t) = \frac{1}{m}\int_0^t e^{\eta(s-t)}f(s)\,ds \tag{6}$$

For the SDE (4), we distinguish two cases:

(1) No damping: If $\eta = 0$, the solution is

$$\tilde{x}(t) = x(t) + \tfrac{\sigma}{m}\textstyle\int_0^t W(s)\,ds \quad , \quad \tilde{v}(t) = v(t) + \tfrac{\sigma}{m}W(t) \tag{7}$$

The integrated Brownian motion has mean zero and variance $\frac{t^3}{3}$, meaning that the expectation and variance of the solutions are

$$\begin{aligned} \mathrm{E}(\tilde{x}(t)) &= x(t) & \mathrm{Var}(\tilde{x}(t)) &= \frac{\sigma^2 t^3}{3m^2} \\ \mathrm{E}(\tilde{v}(t)) &= v(t) & \mathrm{Var}(\tilde{v}(t)) &= \frac{\sigma^2 t}{m^2} \end{aligned} \tag{8}$$

While the stochastic process is centered around the true solution, its variance grows to infinity as time progresses. As a measure of error growth, we use the standard deviation, since it is proportional to the width of the confidence interval for a Gaussian process around its mean:

$$\mathrm{Std}(\tilde{v}(t)) = O(t^{\frac{1}{2}}) \qquad \mathrm{Std}(\tilde{x}(t)) = O(t^{\frac{3}{2}}) \tag{9}$$

(2) Damping: For $\eta > 0$, we obtain

$$\begin{aligned} \tilde{x}(t) &= x(t) + \frac{\sigma}{\eta m}\left(W(t) - \int_0^t e^{\eta(s-t)}dW(s)\right) \\ \tilde{v}(t) &= v(t) + \frac{\sigma}{m}\int_0^t e^{\eta(s-t)}dW(s) \end{aligned} \tag{10}$$

In this case, the velocity consists of a deterministic trend and an Ornstein-Uhlenbeck (mean reversal) process with mean 0. As the latter has bounded variance, the reconstruction of v is merely a question of how accurate the initial measurements are. Unfortunately, the variance of the position is once again unbounded, although it grows more slowly than in the undampened case:

$$\begin{aligned} \mathrm{E}(\tilde{x}(t)) &= x(t) \qquad & \mathrm{Var}(\tilde{x}(t)) &= \frac{\sigma^2}{\eta^2 m^2}\left(t + \frac{1-e^{-2\eta t}}{2\eta} - \frac{2(1-e^{-\eta t})}{\eta}\right) \\ \mathrm{E}(\tilde{v}(t)) &= v(t) \qquad & \mathrm{Var}(\tilde{v}(t)) &= \frac{\sigma^2}{2\eta m^2}(1-e^{-2\eta t}) \end{aligned} \tag{11}$$

Here, we have used the Itô-isometry to calculate

$$\mathrm{Var}\left(\int_0^t e^{\eta(s-t)} dW(s)\right) = \mathrm{E}\left(\left(\int_0^t e^{\eta(s-t)} dW(s)\right)^2\right) = \frac{1-e^{-2\eta t}}{2\eta} \tag{12}$$

To evaluate the variance of $\tilde{x}(t)$, we also need

$$\mathrm{Cov}\left(W(t), \int_0^t e^{\eta(s-t)} dW(s)\right) = \mathrm{E}\left(W(t)\int_0^t e^{\eta(s-t)} dW(s)\right) = \frac{1-e^{-\eta t}}{\eta} \tag{13}$$

where we use the product rule of Itô-calculus to evaluate the product, dropping all stochastic terms as they have mean zero.

In the presence of damping, the standard deviations grow with time as

$$\mathrm{Std}(\tilde{v}(t)) = O(1) \qquad\qquad \mathrm{Std}(\tilde{x}(t)) = O(t^{\frac{1}{2}}) \tag{14}$$

We have seen that even for the simple model (1), a stable (bounded variance) solution exists only if we integrate but once and include a correction term in the equations. Integrating twice will always lead to errors that grow progressively larger over time. The situation can only get worse for a problem involving several bodies, as their relative position and orientation is progressively distorted. This leads to spurious interaction forces and gravity acting in the wrong direction.

It should be noted that the problems caused by noise integration are of principal nature, as there is no way to reconstruct the true forces from the measurements. Preprocessing (e.g. smoothing the data) or more sophisticated integration schemes can reduce the variance σ^2, but this only serves to rescale the error, not bound it.

3 DRIFT CORRECTION

In this section we describe some possible solutions to the drift problem. We consider the case of a full vehicle simulation, which is needed to derive section forces for certain components. The model is unconstrained and excited by measured wheel forces, which are always noisy to some extent. Thus, we have to be aware of a drift of the vehicle body due to the 'Brownian motion effect' described above. Another reason for observing a drift is the fact, that the numerical model is only an approximation of the real vehicle. If, for example, the total mass of the model is too small, then it will lift off during simulation. While the measured wheel forces (up to measurement noise) are 'in equilibrium' with the real vehicle and its motion, this fact need not be true for the numerical model.

First we perform the simulation while ignoring a possible drift and subsequently check the motion of the model. If the observed drift is such that the section forces can be regarded as sufficiently accurate we are done. This is the case if we have a drift in the translational degrees of freedom only. If the drift of the pitch angle (rotation about the lateral axis) and the roll angle (rotation about the longitudinal axis) is too large, we have to assume, that the simulation results are falsified and reject them. We consider the following approaches to deal with the drift:

1. **Artificially constraining the model:** For a vehicle driving over a (possibly rough) horizontal road, we can assume, that the pitch and roll angles are small. Thus, we apply a correction to the simulation as soon as the angles become too large. Sometimes this is accomplished by attaching a rotational spring between the vehicle body and ground, which always tries to keep the angles near zero. While this is a simple workaround, the disadvantages are, that it is not clear how to choose the spring parameters and that undesired reaction torques are induced. The size of these reaction torques can be taken as a measure of validity of this approach: the larger the torques, the more doubtful the results.

   Of course, this approach does not help at all, if the assumption "horizontal road" is not guaranteed, i.e. if we need to simulate curvy, hilly, or even off-road driving. However we will not go into more details.

2. **Additional acceleration sensors:** We use sensors to measure the accelerations at different spots of the vehicle body. This is rather cheap and convenient. These accelerations are used to estimate the motion of the body prior to the simulation. Again we only need to estimate the orientation (rotational degrees of freedom). The approach is described in more detail in Sec. 3.1 below. As we will see, it does not fully solve the drift problem (since two integration steps are needed here too) such that we have to think about additionally measuring quantities at the velocity or even position level.

3. **Additional measurements on the velocity or position levels:** Since both approaches above are not fully satisfying, we have to introduce additional measurements of either (angular) velocities or angles. If the angles of the vehicle body can be measured, we can guide it during the simulation to prevent the drift. If only angular velocities can be measured, we still have to perform one integration to get the angles such that we have to expect small drifts. Sec. 3.2 gives some details of that approach.

3.1 Calculating the rigid body motion from measured accelerations

It is relatively cheap and convenient to measure accelerations at various spots of the vehicle. Here, we investigate how to calculate the body motion of a vehicle from measured accelerations. We assume, that there are $m+1$ sensors at different positions on the body. We introduce the following notation:

x_C, x_i	:	Positions of a reference point C and of the sensors i of the body given in a fixed reference (global frame).
S	:	The transformation from local to global frame. This is the body's orientation in the global frame.
ω, ω_l	:	The angular velocity in the global and local frame.
$r_i, i = 1, \ldots, m+1$	:	The positions of the sensors in the local frame.
$a_i, i = 1, \ldots, m+1$	:	The measured accelerations at position x_i.
$\tilde{a}_i, i = 1, \ldots, m+1$	:	The accelerations at position x_i in the local frame.

$A = [a_1 - a_{m+1}| \dots |a_m - a_{m+1}]$: Matrix of the local relative accelerations.
$R = [r_1 - r_{m+1}| \dots |r_m - r_{m+1}]$: Matrix of the local relative coordinates.

With these notations we have

$$x_i = x_C + S \cdot r_i, i = 1, \dots, m+1. \tag{15}$$

This relation is true only if the body is rigid. Otherwise, we would have to add the deformations. Differentiation and transformation into the local frame gives

$$\tilde{a}_i = S^T \cdot \ddot{x}_i = S^T \cdot \ddot{x}_C + S^T \cdot \ddot{S} \cdot r_i, i = 1, \dots, m+1. \tag{16}$$

By calculating the relative accelerations we eliminate the translational motion and get $\tilde{a}_i - \tilde{a}_{m+1} = S^T \cdot \ddot{S} \cdot (r_i - r_{m+1}), i = 1, \dots, m$. Usually, the sensors are performing a correction with respect to gravity. Since the orientation of the sensors during measurement is unknown, the result of the correction is

$$a_i = \tilde{a}_i + g e_3 - S^T \cdot g e_3, i = 1, \dots, m, \tag{17}$$

where g denotes the gravitational constant and e_3 denotes the direction of gravity (global z-coordinate). For the relative accelerations $a_i - a_{m+1}$ this correction term cancels and we get $A = S^T \cdot \ddot{S} \cdot R$. The matrices R resp. A contain the relative positions resp. accelerations of the first m sensors with respect to the last one. Since the unknown transformation matrix S contains only three degrees of freedom (to be described for instance by Euler or Cardan angles), this matrix equation is an overdetermined set of equations (if m is large enough) for the three parameters. The number of equations depends on the number of sensors. By multiplication with the pseudo inverse (Moore-Penrose inverse) R^+ from the right we get

$$S^T \cdot \ddot{S} = A \cdot R^+. \tag{18}$$

This operation partly removes the redundant accelerations. The remaining equation still contains the inherent consistency condition induced by the fact that the body is non-deformable.

Calculation of the transformation matrix and the angles
By differentiating the identity $\mathbf{I}_3 = S^T \cdot S$ we get

$$S^T \cdot \dot{S} = \tilde{\omega}_l = \begin{pmatrix} 0 & -\omega_{l,3} & \omega_{l,2} \\ \omega_{l,3} & 0 & -\omega_{l,1} \\ -\omega_{l,2} & \omega_{l,1} & 0 \end{pmatrix}, \tag{19}$$

where ω_l denotes the vector of the local angular velocity and $\tilde{\omega}_l$ is the corresponding skew symmetric matrix. Another differentiation leads to

$$S^T \cdot \ddot{S} = \dot{\tilde{\omega}}_l - \tilde{\omega}_l \cdot \tilde{\omega}_l^T = \dot{\tilde{\omega}}_l + \tilde{\omega}_l \cdot \tilde{\omega}_l.$$

and together with (18) we get

$$\dot{\tilde{\omega}}_l + \tilde{\omega}_l \cdot \tilde{\omega}_l = S^T \cdot \ddot{S} = A \cdot R^+ =: M.$$

Since $\dot{\tilde{\omega}}_l$ is skew symmetric and the product $\tilde{\omega}_l \cdot \tilde{\omega}_l$ is symmetric, we have a decomposition of the left-hand side of this equation into a symmetric and a skew symmetric part. Thus, if we define

$$M_- = \tfrac{1}{2}(AR^+ - (AR^+)^T) \quad , \quad M_+ = \tfrac{1}{2}(AR^+ + (AR^+)^T),$$

we have

$$\dot{\tilde{\omega}}_l = M_- \quad , \quad \tilde{\omega}_l \cdot \tilde{\omega}_l = M_+. \tag{20}$$

The first of these relations is a simple set of three uncoupled equations for the local angular velocities and the second one is the consistency condition mentioned above. The transition from A and R^+ to M_- can be interpreted as a projection onto the rigid body motion. Due to possible measurement errors and the deviation from the rigid body motion, we have to take into account large uncertainties in M_-.

In principle, we can use (20) to calculate ω_l by a simple integration. Of course, during integration we have to deal with the accumulation of random errors leading to a drift.

The next step is to calculate the transformation matrix S from the local angular velocities ω_l. To this end, we write S using quaternions in the form

$$S = S(q) = \begin{pmatrix} q_1^2 + q_2^2 - q_3^2 - q_4^2 & 2(q_2q_3 - q_1q_4) & 2(q_2q_4 + q_1q_3) \\ 2(q_2q_3 + q_1q_4) & q_1^2 - q_2^2 + q_3^2 - q_4^2 & 2(q_3q_4 - q_1q_2) \\ 2(q_2q_4 - q_1q_3) & 2(q_3q_4 + q_1q_2) & q_1^2 - q_2^2 - q_3^2 + q_4^2 \end{pmatrix}, \tag{21}$$

where $q = (q_1, q_2, q_3, q_4)^T$ and $||q||^2 = q_1^2 + q_2^2 + q_3^2 + q_4^2 = 1$. Using (19) we arrive at the linear system of equations

$$\dot{q} = \tfrac{1}{2} \cdot \Omega_l \cdot q \quad , \quad \Omega_l = \left(\begin{array}{c|ccc} 0 & -\omega_{l,1} & -\omega_{l,2} & -\omega_{l,3} \\ \hline \omega_{l,1} & 0 & \omega_{l,3} & -\omega_{l,2} \\ \omega_{l,2} & -\omega_{l,3} & 0 & \omega_{l,1} \\ \omega_{l,3} & \omega_{l,2} & -\omega_{l,1} & 0 \end{array}\right) = \left(\begin{array}{c|c} 0 & -\omega_l \\ \hline \omega_l & -\tilde{\omega}_l \end{array}\right). \tag{22}$$

for the quaternions q. Since Ω_l is skew symmetric, the normalisation $||q||^2 = 1$ is preserved during integration. In contrast to other representations of the transformation matrix (Euler or Cardan angles), (22) does not contain singularities and can be integrated over the desired period.

Calculation of the body position

Once the angles α resp. the transformation matrix S are known, we can calculate the body position x_C. Combining (16) and (17), we get

$$\ddot{x}_C = S \cdot \tilde{a}_i - \ddot{S} \cdot r_i = S \cdot (a_i - ge_3) + ge_3 - \ddot{S} \cdot r_i, i = 1, \ldots, m+1.$$

To minimise errors due to the measurement or the deformability, we calculate the mean acceleration

$$\ddot{\bar{x}}_C = \frac{1}{m+1} \sum_{i=1}^{m+1} (S \cdot (a_i - ge_3) + ge_3 - \ddot{S} \cdot r_i). \tag{23}$$

Integrating twice leads to the position x_C. Of course, we will again have a drift during the integration of $\ddot{\bar{x}}_C$. The remaining positions x_i follow from (15).

Summary

The process of calculating the position and orientation of the body from the measured accelerations can be summarised as follows:

1. Calculate the matrix $M_- = \frac{1}{2}(AR^+ - (AR^+)^T)$.

2. Calculate the local angular velocity by integration of $\dot{\tilde{\omega}}_l = M_-$.
3. Calculate the quaternions q by integration of $\dot{q} = \frac{1}{2} \cdot \Omega_l \cdot q$.
4. Calculate the transformation matrix S from (21).
5. Calculate $\ddot{\tilde{x}}_C$ according to (23) and x_C by a twofold integration.
6. Calculate the remaining positions x_i by (15).

Besides drift problems during the integration, this algorithm completely solves the task of calculating the rigid body motion of the car body from measured accelerations.

Remarks

- After the transformation matrix S has been calculated a convenient parametrisation e.g. Euler or Cardan angles can be derived.
- The calculation of the local angular velocities ω_l by integration of $\dot{\tilde{\omega}}_l = M_-$ is the most critical step since the right hand side M_- is disturbed by measurement errors and the fact that the car body is not really rigid. Thus we have to expect a drift in ω_l. If the real vehicle motion during measuring is such that we can assume, that the angular velocities as well as the angles have mean zero and no drift, we can apply a high pass filter to ω_l prior to solving $\dot{q} = \frac{1}{2} \cdot \Omega_l \cdot q$ and again apply a high pass filter to the resulting angles α. However, the final results will depend on the filter parameters (cut-off frequency) and the best choice of parameters is subjective.
- With this approach (just like the "big spring constraint") we still cannot objectively distinguish undesired angular drift from angular movement that may come from a curvy or hilly road.
- A direct measurement of the angular velocities would be much more reliable. The same remarks apply to the calculation of the position by a twofold integration of $\ddot{\tilde{x}}_C$. Again we can apply high pass filtering, but the parameter choice is subjective.
- Nevertheless, the algorithm establishes the relation between the vehicle body motion and accelerations in a rigorous way and at least enables the estimation of the motion in case no additional measurements are available.

3.2 Measurement of angular velocities or angles

We have already argued that for the purpose of calculating section forces, errors in the position of the vehicle are negligible, while its orientation with respect to gravity must be known with sufficient accuracy. An obvious way to improve the quality of a simulation is thus to include measured angles. Typically, these are determined by an inertial navigation system (INS) on board the vehicle. Since an INS uses gyroscopes for measuring angular velocities, any angles reported are derived via integration.

As in Sec. 2, we model the noise on the angular velocities as a Brownian motion with variance $\sigma^2 > 0$. The angular velocities in the local reference frame are replaced by

$$\omega_{l,j} \to \omega_{l,j} + \sigma \, dW_j(t) \tag{24}$$

with independent Brownian motions W_j. Now, the quaternion representation (21) yields the following SDE:

$$d\tilde{q} = \tfrac{1}{2}\Omega_l \tilde{q}\, dt + \tfrac{\sigma}{2}\sum_{j=1}^{3} B_j \tilde{q}\, dW_j(t) \quad , \quad \tilde{q}(0) = q^{(0)} \text{ s.t. } ||q^{(0)}|| = 1 \tag{25}$$

As we are interested in the cumulative effect of measurement noise over time, we do not include an error for the initial value. The matrices B_j correspond to the imaginary units of the quaternions expressed as a subspace of $\mathbb{R}^{4\times4}$:

$$B_1 = \begin{pmatrix} 0 & -1 & 0 & 0 \\ 1 & 0 & 0 & 0 \\ 0 & 0 & 0 & 1 \\ 0 & 0 & -1 & 0 \end{pmatrix} \quad B_2 = \begin{pmatrix} 0 & 0 & -1 & 0 \\ 0 & 0 & 0 & -1 \\ 1 & 0 & 0 & 0 \\ 0 & 1 & 0 & 0 \end{pmatrix} \quad B_3 = \begin{pmatrix} 0 & 0 & 0 & -1 \\ 0 & 0 & 1 & 0 \\ 0 & -1 & 0 & 0 \\ 1 & 0 & 0 & 0 \end{pmatrix} \tag{26}$$

The matrices Ω_l and B_j do not commute under multiplication, so there is no simple closed form solution for (25). To obtain a qualitative understanding of the error dynamics, we consider the simpler problem

$$d\tilde{q} = \tfrac{\sigma}{2} B_j \tilde{q}\, dW_j(t) \quad , \quad \tilde{q}(0) = q^{(0)} \text{ s.t. } ||q^{(0)}|| = 1 \tag{27}$$

with no actual rotation and a single perturbed measurement. The unique solution is

$$\begin{aligned} \tilde{q} &= \exp\left(\frac{\sigma}{2} B_j W_j(t) - \frac{1}{2}\left(\frac{\sigma}{2} B_j\right)^2 t\right) q^{(0)} \\ &= \exp\left(\frac{\sigma^2 t}{8}\right)\left(\cos\left(\frac{\sigma}{2} W_j(t)\right)\mathbf{I}_4 + \sin\left(\frac{\sigma}{2} W_j(t)\right) B_j\right) q^{(0)} \end{aligned} \tag{28}$$

Here, we use the fact that B_j and $\mathbf{I}_4$ commute, as well as the properties

$$B_j^2 = -\mathbf{I}_4 \qquad\qquad \exp(\lambda B_j) = \cos(\lambda)\mathbf{I}_4 + \sin(\lambda) B_j \tag{29}$$

Note that the norm of q grows at an exponential rate, although the exact solution always satisfies $||q(t)|| = 1$. This is a property of the Itô integral, which is replicated if we solve the SDE using the explicit Euler scheme. As we are only interested in the angles, the result is still useful if we normalise q before calculating the rotation matrix. A more satisfying solution would be to use an integration scheme that treats (27) as an SDE in the sense of Stratonovich, as the corresponding solution omits the growth term. However, the usual situation in practice is that neither the ODE nor the solver permit the analysis of error propagation in terms of a simple SDE. The recommended approach in this case is a Monte-Carlo study.

After we normalise the solution of the quaternion equation, its position on the unit sphere is still perturbed by the measurement noise. To see what this means in terms of the rotation matrix S, we first consider the case that $j = 1$ and $q^{(0)}$ is equal to the first unit vector. Equation (21) now yields the following result for $\theta(t) := \frac{\sigma}{2} W_1(t)$:

$$q(t) = \begin{pmatrix} \cos(\theta(t)) \\ \sin(\theta(t)) \\ 0 \\ 0 \end{pmatrix} \Rightarrow S = \begin{pmatrix} 1 & 0 & 0 \\ 0 & \cos(2\theta(t)) & -\sin(2\theta(t)) \\ 0 & \sin(2\theta(t)) & \cos(2\theta(t)) \end{pmatrix} \tag{30}$$

This is a rotation around the x-axis, where the angle behaves like a Brownian motion, so its standard deviation is $O(t^{\frac{1}{2}})$, which we might expect for a single integration step. Analogous

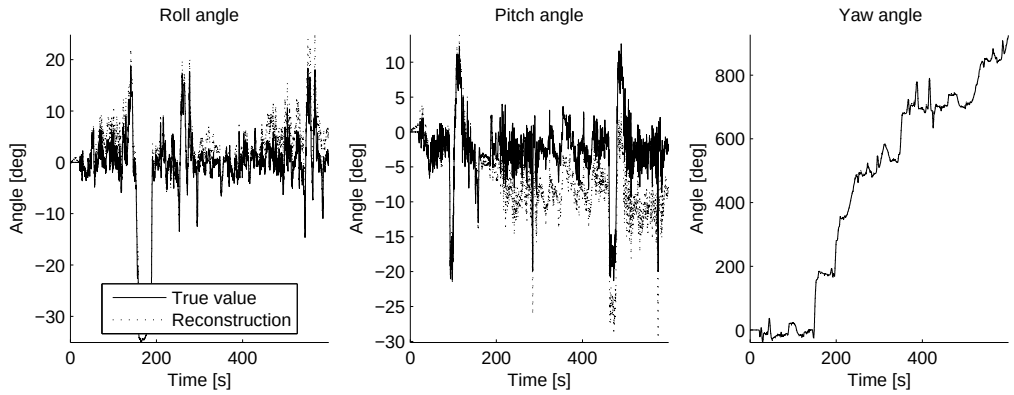

Figure 1: True and reconstructed angles

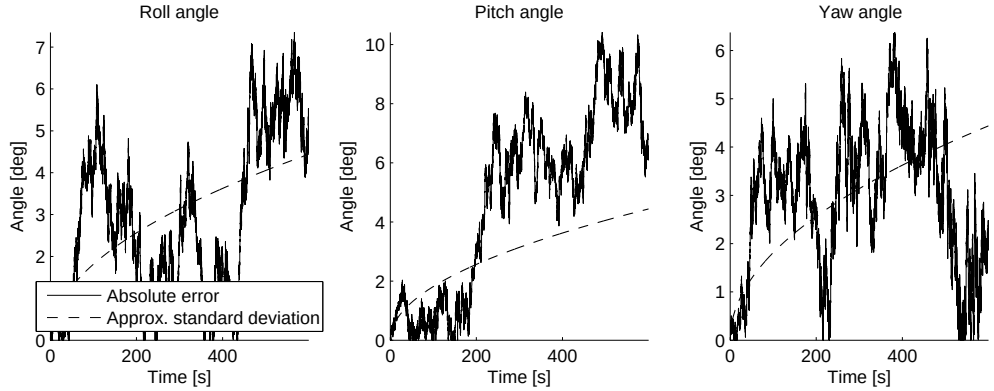

Figure 2: Reconstruction error for angles

calculations for other values of j and i show that distorting (only) $\omega_{l,1}$ always results in a spurious rotation around the x-axis, while $\omega_{l,2}$ affects the y-axis, and $\omega_{l,3}$ the z-axis. We cannot provide an exact solution in the case of three noise terms and non-zero excitation, but the best we may expect are errors growing at the same rate. Thus, including an INS in the process does not solve the problem of noisy data in general. However, short simulations can be stabilised using angular velocities measurements that are sufficiently accurate.

In practice, the accuracy of an INS is affected by other factors besides random noise. For short-term stability, manufacturers often express standard deviation as being linear in operation time (a more detailed analysis may distinguish bias instability of $O(t)$ and angle random walk of $O(t^{\frac{1}{2}})$). The magnitude of these effects can range from below 0.001° per hour for high-performance INS used in aeronautics to over 10° per hour for the cheapest units [12]. To choose the right measuring equipment for a task, one has to know the length of the individual measurements, as well as the sensitivity of the vehicle model to deviations from the true angle. Even an error of 10° per hour can be acceptable for simulating a 5 minute drive.

As a final example, we consider a 10 minute segment of INS data recorded at a frequency of 1000 Hz ($\Delta t = 0.001s$) on board a moving vehicle. Angular velocities were reconstructed by smoothing with a low-pass filter and taking central differences. For the purpose of demonstration, these will be treated as the 'true' values. The angles were reconstructed by solving the quaternion equation (21) with added noise using the DOPRI(4,5) scheme [4]. For the errors, we

used independent Gaussian random variables with mean zero and standard deviation $\sigma_M = 0.1$ radians per second. Taking (5) as a simple approximation, we expect that the angles behave similar to Brownian motion with standard deviation $\sigma = \frac{180^\circ}{\pi}\sigma_M\sqrt{\Delta t} = 0.18\frac{^\circ}{\sqrt{s}}$. As the plots in Figures (1) and (2) show, the errors are indeed of comparable magnitude.

3.3 Stabilising the force-based simulation

In the preceding two sections we have presented how to use additional measurements in order to approximately derive the true trajectory of a certain reference point of the vehicle body. Now, the vehicle motion in the force-based simulation can be stabilised by additionally prescribing the measured motion at the reference point. However, the enforced motion induces reaction forces given by the corresponding Lagrange multipliers. In an ideal situation, where we have nearly no noise in the measured data and a "perfect" model, these reaction forces should be zero.

There is a certain similarity to the Gear-Gupta-Leimkuhler stabilisation for the index reduced formulations of multibody equations (see [6]). The idea of index reduction is to use constraints on the velocity or acceleration level in order to reduce the index of the DAE. But this leads to the well known drift effect of the integration of the pure index 2 or index 1 formulations. This drift can be corrected either by projecting onto the known constraints on position level or by using constraints both on the position as well as on the velocity or acceleration level. To compensate the additional constraints in the latter case, Gear, Gupta, and Leimkuhler introduced corresponding Lagrange multipliers η in the kinematic equation $\dot{x} = v - G^T(x)\eta$. In contrast to our case, no additional forces are introduced by that approach.

Since we are transferring data measured on a real vehicle to a numerical model, the reaction forces observed at the point of the prescribed motion are not only due to the noise in the wheel forces but also due to the fact, that the numerical model is only an approximation of the real vehicle. While for the real vehicle the measured prescribed motion is 'in equilibrium' with the measured wheel forces (up to measurement noise), this need not be true for the numerical model. If, for example, the weight of the vehicle model is too small, then the vertical reaction force will show an offset which is needed to prevent the vehicle model from lifting off during simulation.

If the stabilised simulation is used, one has to check subsequently the magnitude of the artificial reaction forces in order to decide, if the approach is valid (small reaction forces) or not. Of course, in the latter case, it is in general not easy to find out the reason for the mismatch.

4 A SIMPLE EXAMPLE

We want to illustrate the considerations above using the vehicle model shown in Fig. 3. It is taken from Ref. [9]. Although it is simple enough such that the equations of motion can be written down explicitly, it is useful for demonstrating the drift effects explained before. The model contains three bodies (the chassis and two wheels), as well as two spring damper systems between the wheels and the chassis and two additional spring damper systems representing the tyres. The connection between the springs and the chassis is via revolute joints. The chassis moves in vertical direction z_3 (positive z oriented downward) and rotates about the angle β (I denotes the moment of inertia of the chassis). The degrees of freedom of the wheels are z_1, z_2 resp. Thus, the entire system has six degrees of freedom, namely the coordinates of the three bodies z_1, z_2, z_3, β and the coordinates ζ_1, ζ_2 of the contact points to the ground. Details of the model can be found in App. A.

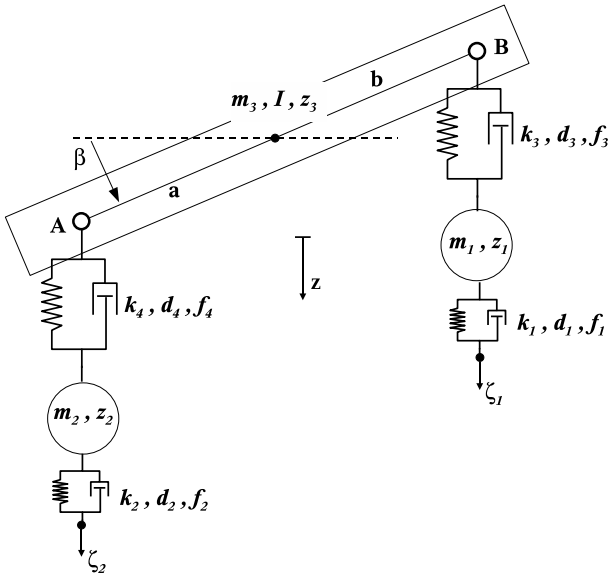

Figure 3: A simple vehicle model.

4.1 Excitation modes of the model

The system may be excited by prescribing either

1. the vertical forces f_1, f_2 at the contact points,
2. the road profile given by ζ_1, ζ_2, or
3. the vertical forces f_1, f_2 and the pitch angle β.

In the first case, the equations of motion may be written in the form

$$M \cdot \dot{x} = A(x) \cdot x + F, \tag{31}$$

where the vector of unknowns x is given by $x = (z_1, z_2, z_3, \beta, \dot{z}_1, \dot{z}_2, \dot{z}_3, \dot{\beta}, \zeta_1, \zeta_2)^T$ and the mass matrix M as well as the system matrix $A(x)$ and the right hand side F is given in App. A.

In the second case, the forces f_1, f_2 at the contact points are reaction forces which are unknown and have to be calculated. The dynamic equations are now given by

$$\bar{M} \cdot \dot{\bar{x}} = \bar{A}(\bar{x}) \cdot \bar{x} + \bar{F}, \tag{32}$$

where the vector of unknowns is given by $\bar{x} = (z_1, z_2, z_3, \beta, \dot{z}_1, \dot{z}_2, \dot{z}_3, \dot{\beta})^T$, and the mass matrix $\bar{M}$ as well as the system matrix $\bar{A}(\bar{x})$ and the right hand side $\bar{F}$ is given in App. A.

After solving these equations for $\bar{x}$, we get the contact forces by

$$\begin{aligned} f_1 &= k_1(\bar{x}_1 - \zeta_1) + d_1(\bar{x}_5 - \dot{\zeta}_1) \\ f_2 &= k_2(\bar{x}_2 - \zeta_2) + d_2(\bar{x}_6 - \dot{\zeta}_2). \end{aligned} \tag{33}$$

In the third case, we stabilise the force-based simulation using the measured pitch angle. Here the vector of unknowns is $\hat{x} = (z_1, z_2, z_3, \dot{z}_1, \dot{z}_2, \dot{z}_3, \zeta_1, \zeta_2)^T$ and the equations of motion are

$$\hat{M} \cdot \dot{\hat{x}} = \hat{A} \cdot \hat{x} + \hat{F}. \tag{34}$$

The mass matrix $\hat{M}$, the system matrix $\hat{A}$, and the right side $\hat{F}$ are given in the appendix. The prescription of the angle β induces an enforced moment λ at the chassis center. Once the equations of motion have been solved, λ can be calculated by

$$\lambda = I\ddot{\beta} - \cos\beta(bf_3 - af_4),$$

where f_3, f_4 are the chassis spring forces defined in (35).

We now use the model to illustrate what may happen if wheel forces measured at a prototype vehicle on a certain track are used for exciting a numerical model (MBS) of the vehicle. Here, we have to replace the measurement by a first simulation of the model based on a predefined road profile ζ_1, ζ_2. The following steps are performed:

1. We simulate the model based on a prescribed road profile. The corresponding equations of motion are given by (32). As a result, we get the vertical wheel forces by (33). We denote these forces by $f_1^{(0)}, f_2^{(0)}$. This step is called **virtual measurement**.

2. We simulate the model using (31), where $f_1 = f_1^{(0)}$ and $f_2 = f_2^{(0)}$. This step is called **simulation based on undisturbed forces**. In the absence of noise and calculation errors, we should get the same vehicle motion as in the virtual measurement.

3. We pretend a **measurement error** by adding a synthetic noise $\varepsilon_1, \varepsilon_2$ to the forces $f_1^{(0)}, f_2^{(0)}$. The noise is stationary with zero mean and variance σ^2. Then we simulate the model using (31), where $f_1 = f_1^{(0)} + \varepsilon_1$ and $f_2 = f_2^{(0)} + \varepsilon_2$. This step is called **simulation based on noisy forces**.

4. We pretend a **modeling error** by slightly changing the stiffness and damping parameters k_3, d_3, k_4, d_4 of the chassis springs as well as the moment of inertia I of the chassis. Then we simulate the modified model using (31) with the unperturbed forces $f_1^{(0)}, f_2^{(0)}$. This step is called **simulation of a perturbed model**. Again we compare the corresponding vehicle motion with the motion from the virtual measurement.

5. We assume, that we have measured the pitch angle β and simulate the perturbed model with the noisy forces under prescription of β using (34). This step is called **stabilised simulation of a perturbed model**.

4.2 Simulation results

The road profile and the wheel forces
In Fig. 4, the road profile used for the virtual measurement and the resulting wheel forces are shown. The profile starts at level zero and ranges approximately between $-2[m]$ and $+2[m]$, simulating some small hill grades. The resulting vertical wheel forces are shown below. They are rather similar for both wheels. Their amplitudes (approximately between $-10[kN]$ and $+16[kN]$) are due to the road roughness, which can be seen in the detail plot of the profile.

Noisy forces and perturbed models
As a model for the measurement error of the forces we have used Gaussian white noise signals $\varepsilon_1, \varepsilon_2$ with standard deviation $\sigma = 0.002 \cdot f_{max}$, where f_{max} is the maximum absolute force. Thus we get $\sigma \approx 32[N]$.

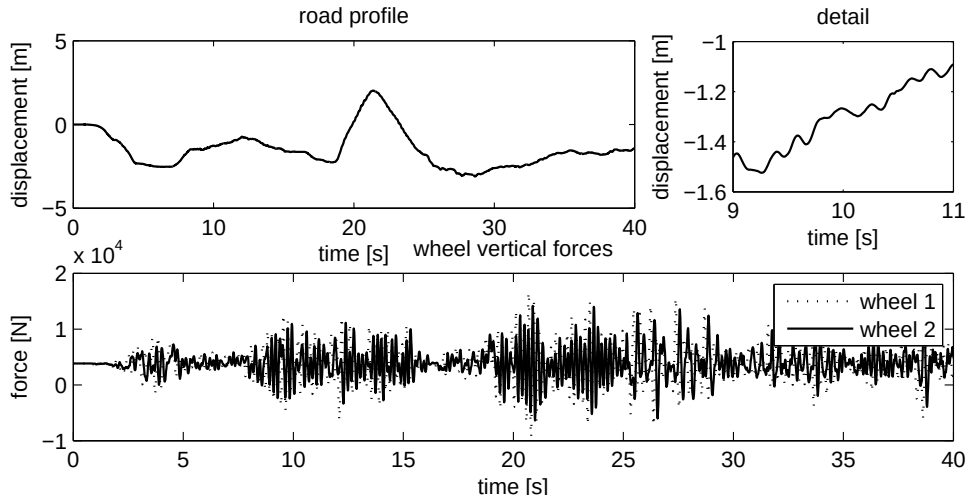

Figure 4: The basic road profile ζ_1, ζ_2 at the top and the resulting wheel forces at the bottom.

When comparing simulation results with the virtual measurement, we only show the vertical chassis motion z_3 and the pitch angle β. The latter is the most sensitive variable. The differences in z_1 and z_2 are smaller in most cases. The virtual measurement is compared to the simulation with undisturbed forces, to the simulation with noisy forces, and to the simulation with the perturbed model. Fig. 5 shows the results for the vertical chassis motion (left) as well as for the

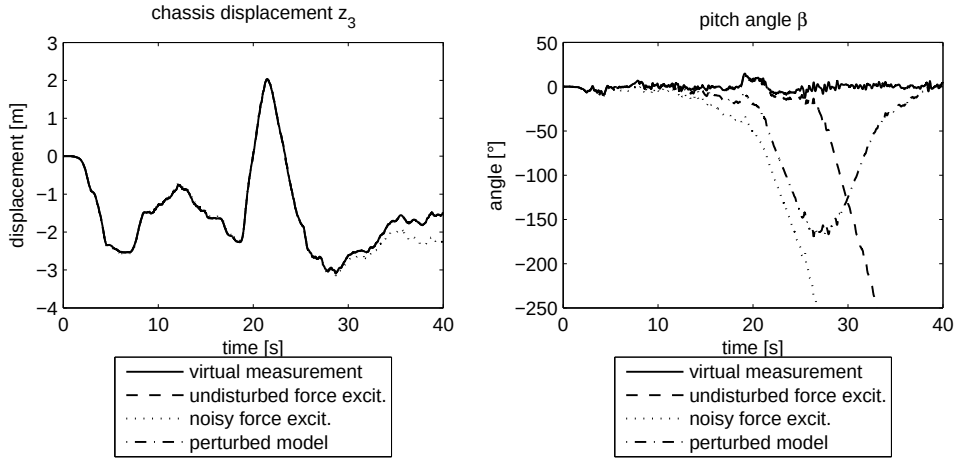

Figure 5: Vertical chassis motion z_3 and pitch angle β during different simulations.

pitch angle (right). There is nearly no drift in z_3 with the exception of the noisy force excitation, where a relatively small drift can be observed. For the pitch angle, even for the simulation with undisturbed forces we observe a drift beyond $20[s]$. As can be expected, the drift-off occurs much earlier (at $10[s]$ approximately) in case of noisy forces or a perturbed model.

In Fig. 6 and Fig. 7 the results for different noise samples and different perturbed models resp. are shown.

While the behaviour of the different noisy force results is pretty similar with respect to the "drift-off" time, the specific trajectories differ a lot. This is in accordance with what can be

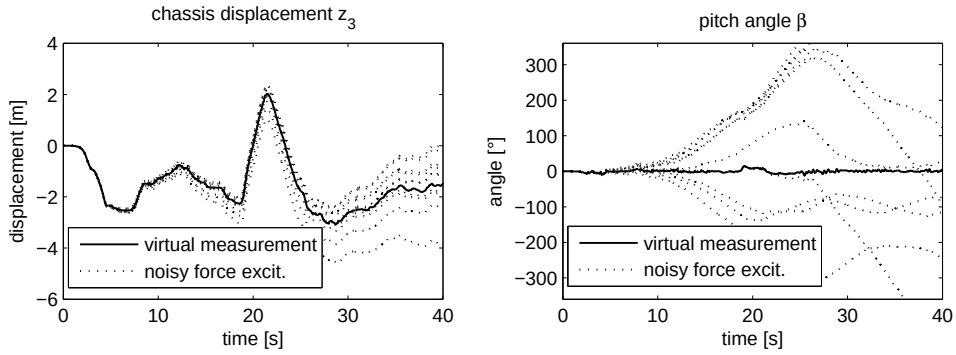

Figure 6: Vertical displacement (left) and pitch angle β (right) of the chassis during force-based excitation for several samples of the noise.

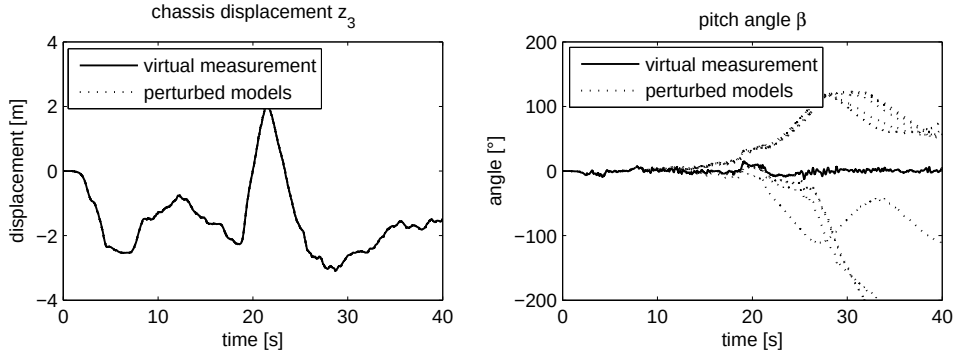

Figure 7: Vertical displacement (left) and pitch angle β (right) of the chassis during force-based excitation for several perturbed models. The perturbation is a random factor between 0.9 and 1.1 (at most 10%) on the stiffness and damping parameters of the chassis springs and on the moment of inertia of the chassis.

observed for multiple paths of the simple point mass example in Sec. 2. In case of the perturbed model we observe nearly no drift in the vertical chassis displacement and different types of drifts for the pitch angle, depending on the specific way, the perturbed model parameters are affecting the physical behaviour.

Prescription of pitch angle

Next we study the effect of prescription of the pitch angle β (stabilisation). When simulating the original model with the prescription of β and undisturbed forces, we get a small enforced moment (not shown) due to small numerical integration errors. In that case its magnitude approximately is $70[Nm]$. If we do the same for the perturbed model and the noisy forces, we have to expect a larger moment. In Fig. 8, the results from the stabilised simulation of the perturbed model excited by the noisy forces are shown. The plot shows the enforced moment (right) and compares it to the inertia term $I \cdot \beta$ (left). The enforced moment approximately ranges between $(-800[Nm], 800[Nm])$, which is considerably larger than in the case without model and force error. However, if we compare the magnitude of the enforced moment with the magnitude of the inertia term $I \cdot \beta$, which approximately is $15[kNm]$, we find that it is relatively small.

The magnitude of the moment can be regarded as a measure of inconsistency between the applied forces, the model, and the enforced motion β. Thus, it should be as small as possible. Of course, in practice it is not known, whether the enforced moment is mainly due to erroneous

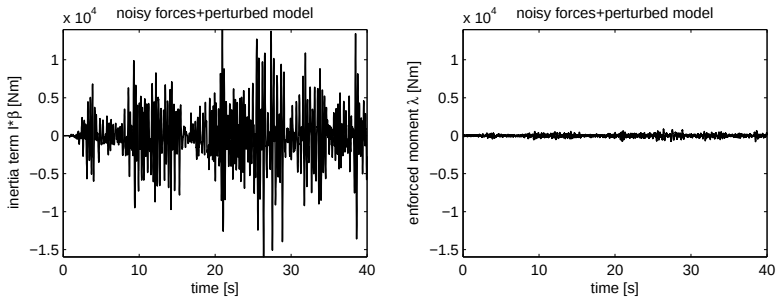

Figure 8: The inertia term $I\beta$ (left) and the moment enforced by the prescription of the pitch angle (right).

forces, model errors or an erroneous prescribed motion.

Remark

For the calculations above the equations of motion given in the appendix have been implemented in MATLAB and solved with different integration schemes (ode45: a Runge-Kutta method by Dormand and Prince, see [4], ode113: a variable order Adams-Bashforth-Moulton method, see [10], ode15s: a variable order solver based on numerical differentiation formulas (NDFs), see [11]) and different error tolerances ($tol_{rel} \in \{10^{-4}, 10^{-8}\}$, $tol_{abs} \in \{10^{-6}, 10^{-10}\}$). It turned out that the presence of the observed drift is essentially independent of the solver and the accuracy of the integration.

5 Conclusions

Starting with some basic observations from the theory of stochastic differential equations, we have argued that the drift effect, observed when simulating unconstrained models based on forces or accelerations, cannot be eliminated by suitable integration schemes. It is a consequence of noise in the excitation data.

The presence of the drift effect even in case of excitation with undisturbed forces is due to small numerical integration errors. Although the magnitude of these errors are under control by setting error tolerances, they may accumulate as has been described in Sec. 2. This can be compared to the well known drift-off, which is observed if DAEs are integrated using the formulation of constraints based on velocity or acceleration levels (hidden constraints). However, in those cases, we can apply stabilisation techniques (e.g. Baumgarte stabilisation, see [2]), since we know the constraints at the position level as well. See [1], [3], or [5] for details on ODE and DAE solving.

As we do not know the true trajectory in our situation, such techniques do not help. The only way around that problem is to stabilise the simulation (Sec. 3.3) making use of data on the position level. Since a pure translational drift would not affect the section forces within the vehicle, we could even do without controlling the translational degrees of freedom and concentrate on the orientation.

As we have seen in Sec. 3.1, we can in principle calculate the orientation from measured accelerations, but during that twofold integration process we again have the same drift problem. Using suitable measurement equipment we can get the angular velocities such that we have to perform only one integration leading to a much smaller drift. It is now a matter of the quality of the measurement equipment to keep the errors sufficiently small. Some of the measurement devices internally perform that integration step and deliver the orientation angles directly. For more details see Sec. 3.2 and the references therein.

Finally in Sec. 4, a simple example has been used to illustrate the considerations.

REFERENCES

[1] U. Ascher, L.R. Petzold. *Computer Methods for Ordinary Differential Equations and Differential–Algebraic Equations*. SIAM, Philadelphia, 1998.

[2] J. Baumgarte. *Stabilization of constraints and integrals of motion in dynamical systems*. Comp. Methods Appl. Mech. 1, 1972, pp 1-16.

[3] K.E. Brenan, S.L. Campbell, L.R. Petzold. *Numerical solution of initial-value problems in differential-algebraic equations*. SIAM, Philadelphia, 2nd edition, 1996.

[4] J.R. Dormand, P. J. Prince. *A family of embedded Runge-Kutta formulae*. J. Comp. Appl. Math., Vol. 6, 1980, pp 19-26.

[5] E. Eich-Soellner, C. Führer. *Numerical Methods in Multibody Dynamics*. Teubner- Verlag, Stuttgart, 1998.

[6] C.W. Gear, G.K. Gupta, B.J. Leimkuhler. *Automatic Integration of the Euler-Lagrange Equations with Constraints*. J. Comp. Appl. Math. 12&13, 1985, pp 77-90.

[7] M.S. Grewal, L.R. Weill, and A.P. Andrews. *Global Positioning Systems, Inertial Navigation, and Integration*. John Wiley & Sons Inc., 2007.

[8] P.E. Kloeden, E. Platen, H. Schurz. *Numerical Solution of SDE Through Computer Experiments*. Springer–Verlag Series Universitext, 2002.

[9] K. Popp and W. Schiehlen. *Ground Vehicle Dynamics – A System Dynamics Approach*. Springer–Verlag Berlin, 2008.

[10] L.F. Shampine, M. K. Gordon. *Computer Solution of Ordinary Differential Equations: the Initial Value Problem*. W. H. Freeman, SanFrancisco, 1975.

[11] L.F. Shampine, M. W. Reichelt. *The MATLAB ODE Suite*. SIAM Journal on Scientific Computing, Vol. 18, 1997, pp 1-22.

[12] D.H. Titterton and J.L. Weston. *Strapdown Inertial Navigation Technology*. The Institution of Electrical Engineers, 2004.

APPENDIX

A The equations of motion of the vehicle model

In the following, the equations of motion of the system are derived. See Fig. 3 for the meaning of the different quantities. We start with the spring forces given by Hook's law and a viscous damping term and the force equilibrium (Newton/Euler equations).

$$\begin{aligned} f_i &= k_i \cdot (z_i - \zeta_i) + d_i \cdot (\dot{z}_i - \dot{\zeta}_i), i = 1, 2 \\ f_3 &= k_3 \cdot (z_3 - z_1 - b \cdot \sin\beta) + d_3 \cdot (\dot{z}_3 - \dot{z}_1 - b \cdot \dot{\beta} \cos\beta) \\ f_4 &= k_4 \cdot (z_3 - z_2 + a \cdot \sin\beta) + d_4 \cdot (\dot{z}_3 - \dot{z}_2 + a \cdot \dot{\beta} \cos\beta) \end{aligned} \tag{35}$$

$$\begin{aligned} m_1 \cdot \ddot{z}_1 = m_1 \cdot g + f_3 - f_1 \quad , \quad m_2 \cdot \ddot{z}_2 = m_2 \cdot g + f_4 - f_2 \\ m_3 \cdot \ddot{z}_3 = m_3 \cdot g - f_3 - f_4 \quad , \quad I \cdot \ddot{\beta} = \cos\beta \cdot (b \cdot f_3 - a \cdot f_4). \end{aligned} \tag{36}$$

Force excitation
Introducing $x = (z_1, z_2, z_3, \beta, \dot{z_1}, \dot{z_2}, \dot{z_3}, \dot{\beta}, \zeta_1, \zeta_2)^T$, combining the formulas (35),(36), and rearranging terms results in the following first order system of differential equations:

$$
\begin{aligned}
M\dot{x} &= A(x) \cdot x + F, \qquad M = \mathrm{diag}(1,1,1,1,m_1,m_2,m_3,I,d_1,d_2),\\
F &= (0,0,0,0,m_1g - f_1, m_2g - f_2, m_3g, 0, -f_1, -f_2)^T,\\
A &= \begin{pmatrix} 0 & \mathbf{I}_4 & 0 \\ A_{21} & A_{22} & 0 \\ A_{31} & A_{32} & A_{33} \end{pmatrix},\\
A_{21} &= \begin{pmatrix} -k_3 & 0 & k_3 & -bk_3\frac{\sin x_4}{x_4} \\ 0 & -k_4 & k_4 & ak_4\frac{\sin x_4}{x_4} \\ k_3 & k_4 & -k_3-k_4 & (bk_3-ak_4)\frac{\sin x_4}{x_4} \\ -bk_3\cos x_4 & ak_4\cos x_4 & (bk_3-ak_4)\cos x_4 & (-b^2k_3-a^2k_4)\cos x_4\frac{\sin x_4}{x_4} \end{pmatrix}, \qquad (37)\\
A_{22} &= \begin{pmatrix} -d_3 & 0 & d_3 & -bd_3\cos x_4 \\ 0 & -d_4 & d_4 & ad_4\cos x_4 \\ d_3 & d_4 & -d_3-d_4 & (bd_3-ad_4)\cos x_4 \\ -bd_3\cos x_4 & ad_4\cos x_4 & (bd_3-ad_4)\cos x_4 & (-b^2d_3-a^2d_4)\cos^2 x_4 \end{pmatrix},\\
A_{31} &= \begin{pmatrix} k_1 & 0 & 0 & 0 \\ 0 & k_2 & 0 & 0 \end{pmatrix}, A_{32} = \begin{pmatrix} d_1 & 0 & 0 & 0 \\ 0 & d_2 & 0 & 0 \end{pmatrix}, A_{33} = \begin{pmatrix} -k_1 & 0 \\ 0 & -k_2 \end{pmatrix}.
\end{aligned}
$$

Eq. (37) describes the system excited by the forces f_1, f_2 at the contact points to the ground. The system matrix $A(x)$ depends on the pitch angle only ($A(x) = A(x_4) = A(\beta)$). For small angles β we have $\cos\beta \approx 1$ and $\frac{\sin\beta}{\beta} \approx 1$, such that the vehicle can be described by a linear system $M \cdot \dot{x} = A(0) \cdot x + F$.

Excitation by a road profile
If the system is excited by a given road profile ζ_1, ζ_2 , then the forces f_1, f_2 at the contact points are reaction forces which are unknown prior to simulation. In that case the dynamic equations are given by

$$
\begin{aligned}
\bar{M}\dot{\bar{x}} &= \bar{A}(\bar{x}) \cdot \bar{x} + \bar{F}, \qquad \bar{M} = \mathrm{diag}(1,1,1,1,m_1,m_2,m_3,I),\\
\bar{F} &= (0,0,0,0,m_1g + k_1\zeta_1 + d_1\dot{\zeta_1}, m_2g + k_2\zeta_2 + d_2\dot{\zeta_2}, m_3g, 0)^T,\\
\bar{A} &= \begin{pmatrix} 0 & \mathbf{I}_4 \\ \bar{A}_{21} & \bar{A}_{22} \end{pmatrix}, \bar{A}_{21} = A_{21} - \begin{pmatrix} k_1 & 0 & 0 & 0 \\ 0 & k_2 & 0 & 0 \\ 0 & 0 & 0 & 0 \\ 0 & 0 & 0 & 0 \end{pmatrix}, \bar{A}_{22} = A_{22} - \begin{pmatrix} d_1 & 0 & 0 & 0 \\ 0 & d_2 & 0 & 0 \\ 0 & 0 & 0 & 0 \\ 0 & 0 & 0 & 0 \end{pmatrix}.
\end{aligned} \qquad (38)
$$

where the vector of unknowns $\bar{x}$ is given by $\bar{x} = (z_1, z_2, z_3, \beta, \dot{z_1}, \dot{z_2}, \dot{z_3}, \dot{\beta})^T$.

A.1 Force excitation with prescribed pitch angle

If we prescribe the pitch angle β during force excitation f_1, f_2 , we get an enforced moment λ at the center of mass of body 3. Since β is no longer an unknown, we introduce the new

variable vector $\hat{x} = (z_1, z_2, z_3, \dot{z}_1, \dot{z}_2, \dot{z}_3, \zeta_1, \zeta_2)^T$. Skipping the β-rows of matrix $A(x)$ in (37) and putting the β-columns into the new force vector $\hat{F}$ leads to

$$\hat{M}\dot{\hat{x}} = \hat{A} \cdot \hat{x} + \hat{F}, \qquad \hat{M} = \mathrm{diag}(1, 1, 1, m_1, m_2, m_3, d_1, d_2),$$

$$\hat{F} = \begin{pmatrix} 0 \\ 0 \\ 0 \\ m_1 g - f_1 - k_3 b \sin\beta - d_3 b \dot{\beta} \cos\beta \\ m_2 g - f_2 + k_4 a \sin\beta + d_4 a \dot{\beta} \cos\beta \\ m_3 g + (k_3 b - k_4 a) \sin\beta + (d_3 b - d_4 a) \dot{\beta} \cos\beta \\ -f_1 \\ -f_2 \end{pmatrix}, \tag{39}$$

$$\hat{A} = \begin{pmatrix} 0 & 0 & 0 & 1 & 0 & 0 & 0 & 0 \\ 0 & 0 & 0 & 0 & 1 & 0 & 0 & 0 \\ 0 & 0 & 0 & 0 & 0 & 1 & 0 & 0 \\ -k_3 & 0 & k_3 & -d_3 & 0 & d_3 & 0 & 0 \\ 0 & -k_4 & k_4 & 0 & -d_4 & d_4 & 0 & 0 \\ k_3 & k_4 & -k_3 - k_4 & d_3 & d_4 & -d_3 - d_4 & 0 & 0 \\ k_1 & 0 & 0 & d_1 & 0 & 0 & -k_1 & 0 \\ 0 & k_2 & 0 & 0 & d_2 & 0 & 0 & -k_2 \end{pmatrix}.$$

The system matrix $\hat{A}$ does no longer depend on the unknown states $\hat{x}$. Thus, the vehicle excited by the contact forces and guided by the prescription of β is represented by a linear model.

B Model parameters

The following parameters are used:

geometry	inertia	stiffness $[N/m]$	damping $[Ns/m]$
$a = 1[m]$	$m_1 = 15[kg]$	$k_1 = 2 \cdot 10^5$	$d_1 = 2 \cdot 10^2$
$b = 1[m]$	$m_2 = 15[kg]$	$k_2 = 2 \cdot 10^5$	$d_2 = 2 \cdot 10^2$
	$m_3 = 750[kg]$	$k_3 = 1 \cdot 10^5$	$d_3 = 1 \cdot 10^4$
	$I = 500[kgm^2]$	$k_4 = 1 \cdot 10^5$	$d_4 = 1 \cdot 10^4$

For the perturbed model, the stiffness and damping of the chassis springs as well as the moment of inertia of the chassis have been changed according to

$$k_3 \leftarrow k_3 \cdot 1.05, \quad k_4 \leftarrow k_4 \cdot 0.95, \quad d_3 \leftarrow d_3 \cdot 0.95, \quad d_4 \leftarrow d_4 \cdot 1.05, \quad I \leftarrow I \cdot 0.95.$$

Published reports of the Fraunhofer ITWM

The PDF-files of the following reports are available under:
www.itwm.fraunhofer.de/de/zentral__berichte/berichte

1. D. Hietel, K. Steiner, J. Struckmeier
A Finite - Volume Particle Method for Compressible Flows
(19 pages, 1998)

2. M. Feldmann, S. Seibold
Damage Diagnosis of Rotors: Application of Hilbert Transform and Multi-Hypothesis Testing
Keywords: Hilbert transform, damage diagnosis, Kalman filtering, non-linear dynamics
(23 pages, 1998)

3. Y. Ben-Haim, S. Seibold
Robust Reliability of Diagnostic Multi-Hypothesis Algorithms: Application to Rotating Machinery
Keywords: Robust reliability, convex models, Kalman filtering, multi-hypothesis diagnosis, rotating machinery, crack diagnosis
(24 pages, 1998)

4. F.-Th. Lentes, N. Siedow
Three-dimensional Radiative Heat Transfer in Glass Cooling Processes
(23 pages, 1998)

5. A. Klar, R. Wegener
A hierarchy of models for multilane vehicular traffic
Part I: Modeling
(23 pages, 1998)

Part II: Numerical and stochastic investigations
(17 pages, 1998)

6. A. Klar, N. Siedow
Boundary Layers and Domain Decomposition for Radiative Heat Transfer and Diffusion Equations: Applications to Glass Manufacturing Processes
(24 pages, 1998)

7. I. Choquet
Heterogeneous catalysis modelling and numerical simulation in rarified gas flows Part I: Coverage locally at equilibrium
(24 pages, 1998)

8. J. Ohser, B. Steinbach, C. Lang
Efficient Texture Analysis of Binary Images
(17 pages, 1998)

9. J. Orlik
Homogenization for viscoelasticity of the integral type with aging and shrinkage
(20 pages, 1998)

10. J. Mohring
Helmholtz Resonators with Large Aperture
(21 pages, 1998)

11. H. W. Hamacher, A. Schöbel
On Center Cycles in Grid Graphs
(15 pages, 1998)

12. H. W. Hamacher, K.-H. Küfer
Inverse radiation therapy planning - a multiple objective optimisation approach
(14 pages, 1999)

13. C. Lang, J. Ohser, R. Hilfer
On the Analysis of Spatial Binary Images
(20 pages, 1999)

14. M. Junk
On the Construction of Discrete Equilibrium Distributions for Kinetic Schemes
(24 pages, 1999)

15. M. Junk, S. V. Raghurame Rao
A new discrete velocity method for Navier-Stokes equations
(20 pages, 1999)

16. H. Neunzert
Mathematics as a Key to Key Technologies
(39 pages (4 PDF-Files), 1999)

17. J. Ohser, K. Sandau
Considerations about the Estimation of the Size Distribution in Wicksell's Corpuscle Problem
(18 pages, 1999)

18. E. Carrizosa, H. W. Hamacher, R. Klein, S. Nickel
Solving nonconvex planar location problems by finite dominating sets
Keywords: Continuous Location, Polyhedral Gauges, Finite Dominating Sets, Approximation, Sandwich Algorithm, Greedy Algorithm
(19 pages, 2000)

19. A. Becker
A Review on Image Distortion Measures
Keywords: Distortion measure, human visual system
(26 pages, 2000)

20. H. W. Hamacher, M. Labbé, S. Nickel, T. Sonneborn
Polyhedral Properties of the Uncapacitated Multiple Allocation Hub Location Problem
Keywords: integer programming, hub location, facility location, valid inequalities, facets, branch and cut
(21 pages, 2000)

21. H. W. Hamacher, A. Schöbel
Design of Zone Tariff Systems in Public Transportation
(30 pages, 2001)

22. D. Hietel, M. Junk, R. Keck, D. Teleaga
The Finite-Volume-Particle Method for Conservation Laws
(16 pages, 2001)

23. T. Bender, H. Hennes, J. Kalcsics, M. T. Melo, S. Nickel
Location Software and Interface with GIS and Supply Chain Management
Keywords: facility location, software development, geographical information systems, supply chain management
(48 pages, 2001)

24. H. W. Hamacher, S. A. Tjandra
Mathematical Modelling of Evacuation Problems: A State of Art
(44 pages, 2001)

25. J. Kuhnert, S. Tiwari
Grid free method for solving the Poisson equation
Keywords: Poisson equation, Least squares method, Grid free method
(19 pages, 2001)

26. T. Götz, H. Rave, D. Reinel-Bitzer, K. Steiner, H. Tiemeier
Simulation of the fiber spinning process
Keywords: Melt spinning, fiber model, Lattice Boltzmann, CFD
(19 pages, 2001)

27. A. Zemitis
On interaction of a liquid film with an obstacle
Keywords: impinging jets, liquid film, models, numerical solution, shape
(22 pages, 2001)

28. I. Ginzburg, K. Steiner
Free surface lattice-Boltzmann method to model the filling of expanding cavities by Bingham Fluids
Keywords: Generalized LBE, free-surface phenomena, interface boundary conditions, filling processes, Bingham viscoplastic model, regularized models
(22 pages, 2001)

29. H. Neunzert
»Denn nichts ist für den Menschen als Menschen etwas wert, was er nicht mit Leidenschaft tun kann«
Vortrag anlässlich der Verleihung des Akademiepreises des Landes Rheinland-Pfalz am 21.11.2001
Keywords: Lehre, Forschung, angewandte Mathematik, Mehrskalenanalyse, Strömungsmechanik
(18 pages, 2001)

30. J. Kuhnert, S. Tiwari
Finite pointset method based on the projection method for simulations of the incompressible Navier-Stokes equations
Keywords: Incompressible Navier-Stokes equations, Meshfree method, Projection method, Particle scheme, Least squares approximation
AMS subject classification: 76D05, 76M28
(25 pages, 2001)

31. R. Korn, M. Krekel
Optimal Portfolios with Fixed Consumption or Income Streams
Keywords: Portfolio optimisation, stochastic control, HJB equation, discretisation of control problems
(23 pages, 2002)

32. M. Krekel
Optimal portfolios with a loan dependent credit spread
Keywords: Portfolio optimisation, stochastic control, HJB equation, credit spread, log utility, power utility, non-linear wealth dynamics
(25 pages, 2002)

33. J. Ohser, W. Nagel, K. Schladitz
The Euler number of discretized sets – on the choice of adjacency in homogeneous lattices
Keywords: image analysis, Euler number, neighborhod relationships, cuboidal lattice
(32 pages, 2002)

34. I. Ginzburg, K. Steiner
Lattice Boltzmann Model for Free-Surface flow and Its Application to Filling Process in Casting

Keywords: Lattice Boltzmann models; free-surface phenomena; interface boundary conditions; filling processes; injection molding; volume of fluid method; interface boundary conditions; advection-schemes; upwind-schemes
(54 pages, 2002)

35. M. Günther, A. Klar, T. Materne, R. Wegener
Multivalued fundamental diagrams and stop and go waves for continuum traffic equations
Keywords: traffic flow, macroscopic equations, kinetic derivation, multivalued fundamental diagram, stop and go waves, phase transitions
(25 pages, 2002)

36. S. Feldmann, P. Lang, D. Prätzel-Wolters
Parameter influence on the zeros of network determinants
Keywords: Networks, Equicofactor matrix polynomials, Realization theory, Matrix perturbation theory
(30 pages, 2002)

37. K. Koch, J. Ohser, K. Schladitz
Spectral theory for random closed sets and estimating the covariance via frequency space
Keywords: Random set, Bartlett spectrum, fast Fourier transform, power spectrum
(28 pages, 2002)

38. D. d'Humières, I. Ginzburg
Multi-reflection boundary conditions for lattice Boltzmann models
Keywords: lattice Boltzmann equation, boudary condistions, bounce-back rule, Navier-Stokes equation
(72 pages, 2002)

39. R. Korn
Elementare Finanzmathematik
Keywords: Finanzmathematik, Aktien, Optionen, Portfolio-Optimierung, Börse, Lehrerweiterbildung, Mathematikunterricht
(98 pages, 2002)

40. J. Kallrath, M. C. Müller, S. Nickel
Batch Presorting Problems: Models and Complexity Results
Keywords: Complexity theory, Integer programming, Assigment, Logistics
(19 pages, 2002)

41. J. Linn
On the frame-invariant description of the phase space of the Folgar-Tucker equation
Key words: fiber orientation, Folgar-Tucker equation, injection molding
(5 pages, 2003)

42. T. Hanne, S. Nickel
A Multi-Objective Evolutionary Algorithm for Scheduling and Inspection Planning in Software Development Projects
Key words: multiple objective programming, project management and scheduling, software development, evolutionary algorithms, efficient set
(29 pages, 2003)

43. T. Bortfeld , K.-H. Küfer, M. Monz, A. Scherrer, C. Thieke, H. Trinkaus
Intensity-Modulated Radiotherapy - A Large Scale Multi-Criteria Programming Problem
Keywords: multiple criteria optimization, representative systems of Pareto solutions, adaptive triangulation, clustering and disaggregation techniques, visualization of Pareto solutions, medical physics, external beam radiotherapy planning, intensity modulated radiotherapy
(31 pages, 2003)

44. T. Halfmann, T. Wichmann
Overview of Symbolic Methods in Industrial Analog Circuit Design
Keywords: CAD, automated analog circuit design, symbolic analysis, computer algebra, behavioral modeling, system simulation, circuit sizing, macro modeling, differential-algebraic equations, index
(17 pages, 2003)

45. S. E. Mikhailov, J. Orlik
Asymptotic Homogenisation in Strength and Fatigue Durability Analysis of Composites
Keywords: multiscale structures, asymptotic homogenization, strength, fatigue, singularity, non-local conditions
(14 pages, 2003)

46. P. Domínguez-Marín, P. Hansen, N. Mladenovi´c , S. Nickel
Heuristic Procedures for Solving the Discrete Ordered Median Problem
Keywords: genetic algorithms, variable neighborhood search, discrete facility location
(31 pages, 2003)

47. N. Boland, P. Domínguez-Marín, S. Nickel, J. Puerto
Exact Procedures for Solving the Discrete Ordered Median Problem
Keywords: discrete location, Integer programming
(41 pages, 2003)

48. S. Feldmann, P. Lang
Padé-like reduction of stable discrete linear systems preserving their stability
Keywords: Discrete linear systems, model reduction, stability, Hankel matrix, Stein equation
(16 pages, 2003)

49. J. Kallrath, S. Nickel
A Polynomial Case of the Batch Presorting Problem
Keywords: batch presorting problem, online optimization, competetive analysis, polynomial algorithms, logistics
(17 pages, 2003)

50. T. Hanne, H. L. Trinkaus
knowCube for MCDM – Visual and Interactive Support for Multicriteria Decision Making
Key words: Multicriteria decision making, knowledge management, decision support systems, visual interfaces, interactive navigation, real-life applications.
(26 pages, 2003)

51. O. Iliev, V. Laptev
On Numerical Simulation of Flow Through Oil Filters
Keywords: oil filters, coupled flow in plain and porous media, Navier-Stokes, Brinkman, numerical simulation
(8 pages, 2003)

52. W. Dörfler, O. Iliev, D. Stoyanov, D. Vassileva
On a Multigrid Adaptive Refinement Solver for Saturated Non-Newtonian Flow in Porous Media
Keywords: Nonlinear multigrid, adaptive refinement, non-Newtonian flow in porous media
(17 pages, 2003)

53. S. Kruse
On the Pricing of Forward Starting Options under Stochastic Volatility
Keywords: Option pricing, forward starting options, Heston model, stochastic volatility, cliquet options
(11 pages, 2003)

54. O. Iliev, D. Stoyanov
Multigrid – adaptive local refinement solver for incompressible flows
Keywords: Navier-Stokes equations, incompressible flow, projection-type splitting, SIMPLE, multigrid methods, adaptive local refinement, lid-driven flow in a cavity
(37 pages, 2003)

55. V. Starikovicius
The multiphase flow and heat transfer in porous media
Keywords: Two-phase flow in porous media, various formulations, global pressure, multiphase mixture model, numerical simulation
(30 pages, 2003)

56. P. Lang, A. Sarishvili, A. Wirsen
Blocked neural networks for knowledge extraction in the software development process
Keywords: Blocked Neural Networks, Nonlinear Regression, Knowledge Extraction, Code Inspection
(21 pages, 2003)

57. H. Knaf, P. Lang, S. Zeiser
Diagnosis aiding in Regulation Thermography using Fuzzy Logic
Keywords: fuzzy logic,knowledge representation, expert system
(22 pages, 2003)

58. M. T. Melo, S. Nickel, F. Saldanha da Gama
Largescale models for dynamic multicommodity capacitated facility location
Keywords: supply chain management, strategic planning, dynamic location, modeling
(40 pages, 2003)

59. J. Orlik
Homogenization for contact problems with periodically rough surfaces
Keywords: asymptotic homogenization, contact problems
(28 pages, 2004)

60. A. Scherrer, K.-H. Küfer, M. Monz, F. Alonso, T. Bortfeld
IMRT planning on adaptive volume structures – a significant advance of computational complexity
Keywords: Intensity-modulated radiation therapy (IMRT), inverse treatment planning, adaptive volume structures, hierarchical clustering, local refinement, adaptive clustering, convex programming, mesh generation, multi-grid methods
(24 pages, 2004)

61. D. Kehrwald
Parallel lattice Boltzmann simulation of complex flows
Keywords: Lattice Boltzmann methods, parallel computing, microstructure simulation, virtual material design, pseudo-plastic fluids, liquid composite moulding
(12 pages, 2004)

62. O. Iliev, J. Linn, M. Moog, D. Niedziela, V. Starikovicius
On the Performance of Certain Iterative Solvers for Coupled Systems Arising in Discretization of Non-Newtonian Flow Equations
Keywords: Performance of iterative solvers, Preconditioners, Non-Newtonian flow
(17 pages, 2004)

63. R. Ciegis, O. Iliev, S. Rief, K. Steiner
On Modelling and Simulation of Different Regimes for Liquid Polymer Moulding

Keywords: Liquid Polymer Moulding, Modelling, Simulation, Infiltration, Front Propagation, non-Newtonian flow in porous media
(43 pages, 2004)

64. T. Hanne, H. Neu
Simulating Human Resources in Software Development Processes
Keywords: Human resource modeling, software process, productivity, human factors, learning curve
(14 pages, 2004)

65. O. Iliev, A. Mikelic, P. Popov
Fluid structure interaction problems in deformable porous media: Toward permeability of deformable porous media
Keywords: fluid-structure interaction, deformable porous media, upscaling, linear elasticity, stokes, finite elements
(28 pages, 2004)

66. F. Gaspar, O. Iliev, F. Lisbona, A. Naumovich, P. Vabishchevich
On numerical solution of 1-D poroelasticity equations in a multilayered domain
Keywords: poroelasticity, multilayered material, finite volume discretization, MAC type grid
(41 pages, 2004)

67. J. Ohser, K. Schladitz, K. Koch, M. Nöthe
Diffraction by image processing and its application in materials science
Keywords: porous microstructure, image analysis, random set, fast Fourier transform, power spectrum, Bartlett spectrum
(13 pages, 2004)

68. H. Neunzert
Mathematics as a Technology: Challenges for the next 10 Years
Keywords: applied mathematics, technology, modelling, simulation, visualization, optimization, glass processing, spinning processes, fiber-fluid interaction, trubulence effects, topological optimization, multicriteria optimization, Uncertainty and Risk, financial mathematics, Malliavin calculus, Monte-Carlo methods, virtual material design, filtration, bio-informatics, system biology
(29 pages, 2004)

69. R. Ewing, O. Iliev, R. Lazarov, A. Naumovich
On convergence of certain finite difference discretizations for 1D poroelasticity interface problems
Keywords: poroelasticity, multilayered material, finite volume discretizations, MAC type grid, error estimates
(26 pages,2004)

70. W. Dörfler, O. Iliev, D. Stoyanov, D. Vassileva
On Efficient Simulation of Non-Newtonian Flow in Saturated Porous Media with a Multigrid Adaptive Refinement Solver
Keywords: Nonlinear multigrid, adaptive renement, non-Newtonian in porous media
(25 pages, 2004)

71. J. Kalcsics, S. Nickel, M. Schröder
Towards a Unified Territory Design Approach – Applications, Algorithms and GIS Integration
Keywords: territory desgin, political districting, sales territory alignment, optimization algorithms, Geographical Information Systems
(40 pages, 2005)

72. K. Schladitz, S. Peters, D. Reinel-Bitzer, A. Wiegmann, J. Ohser
Design of acoustic trim based on geometric modeling and flow simulation for non-woven
Keywords: random system of fibers, Poisson line process, flow resistivity, acoustic absorption, Lattice-Boltzmann method, non-woven
(21 pages, 2005)

73. V. Rutka, A. Wiegmann
Explicit Jump Immersed Interface Method for virtual material design of the effective elastic moduli of composite materials
Keywords: virtual material design, explicit jump immersed interface method, effective elastic moduli, composite materials
(22 pages, 2005)

74. T. Hanne
Eine Übersicht zum Scheduling von Baustellen
Keywords: Projektplanung, Scheduling, Bauplanung, Bauindustrie
(32 pages, 2005)

75. J. Linn
The Folgar-Tucker Model as a Differetial Algebraic System for Fiber Orientation Calculation
Keywords: fiber orientation, Folgar–Tucker model, invariants, algebraic constraints, phase space, trace stability
(15 pages, 2005)

76. M. Speckert, K. Dreßler, H. Mauch, A. Lion, G. J. Wierda
Simulation eines neuartigen Prüfsystems für Achserprobungen durch MKS-Modellierung einschließlich Regelung
Keywords: virtual test rig, suspension testing, multibody simulation, modeling hexapod test rig, optimization of test rig configuration
(20 pages, 2005)

77. K.-H. Küfer, M. Monz, A. Scherrer, P. Süss, F. Alonso, A. S. A. Sultan, Th. Bortfeld, D. Craft, Chr. Thieke
Multicriteria optimization in intensity modulated radiotherapy planning
Keywords: multicriteria optimization, extreme solutions, real-time decision making, adaptive approximation schemes, clustering methods, IMRT planning, reverse engineering
(51 pages, 2005)

78. S. Amstutz, H. Andrä
A new algorithm for topology optimization using a level-set method
Keywords: shape optimization, topology optimization, topological sensitivity, level-set
(22 pages, 2005)

79. N. Ettrich
Generation of surface elevation models for urban drainage simulation
Keywords: Flooding, simulation, urban elevation models, laser scanning
(22 pages, 2005)

80. H. Andrä, J. Linn, I. Matei, I. Shklyar, K. Steiner, E. Teichmann
OPTCAST – Entwicklung adäquater Strukturoptimierungsverfahren für Gießereien Technischer Bericht (KURZFASSUNG)
Keywords: Topologieoptimierung, Level-Set-Methode, Gießprozesssimulation, Gießtechnische Restriktionen, CAE-Kette zur Strukturoptimierung
(77 pages, 2005)

81. N. Marheineke, R. Wegener
Fiber Dynamics in Turbulent Flows Part I: General Modeling Framework
Keywords: fiber-fluid interaction; Cosserat rod; turbulence modeling; Kolmogorov's energy spectrum; double-velocity correlations; differentiable Gaussian fields
(20 pages, 2005)

Part II: Specific Taylor Drag
Keywords: flexible fibers; k-ε turbulence model; fiber-turbulence interaction scales; air drag; random Gaussian aerodynamic force; white noise; stochastic differential equations; ARMA process
(18 pages, 2005)

82. C. H. Lampert, O. Wirjadi
An Optimal Non-Orthogonal Separation of the Anisotropic Gaussian Convolution Filter
Keywords: Anisotropic Gaussian filter, linear filtering, orientation space, nD image processing, separable filters
(25 pages, 2005)

83. H. Andrä, D. Stoyanov
Error indicators in the parallel finite element solver for linear elasticity DDFEM
Keywords: linear elasticity, finite element method, hierarchical shape functions, domain decom-position, parallel implementation, a posteriori error estimates
(21 pages, 2006)

84. M. Schröder, I. Solchenbach
Optimization of Transfer Quality in Regional Public Transit
Keywords: public transit, transfer quality, quadratic assignment problem
(16 pages, 2006)

85. A. Naumovich, F. J. Gaspar
On a multigrid solver for the three-dimensional Biot poroelasticity system in multilayered domains
Keywords: poroelasticity, interface problem, multigrid, operator-dependent prolongation
(11 pages, 2006)

86. S. Panda, R. Wegener, N. Marheineke
Slender Body Theory for the Dynamics of Curved Viscous Fibers
Keywords: curved viscous fibers; fluid dynamics; Navier-Stokes equations; free boundary value problem; asymptotic expansions; slender body theory
(14 pages, 2006)

87. E. Ivanov, H. Andrä, A. Kudryavtsev
Domain Decomposition Approach for Automatic Parallel Generation of Tetrahedral Grids
Key words: Grid Generation, Unstructured Grid, Delaunay Triangulation, Parallel Programming, Domain Decomposition, Load Balancing
(18 pages, 2006)

88. S. Tiwari, S. Antonov, D. Hietel, J. Kuhnert, R. Wegener
A Meshfree Method for Simulations of Interactions between Fluids and Flexible Structures
Key words: Meshfree Method, FPM, Fluid Structure Interaction, Sheet of Paper, Dynamical Coupling
(16 pages, 2006)

89. R. Ciegis , O. Iliev, V. Starikovicius, K. Steiner
Numerical Algorithms for Solving Problems of Multiphase Flows in Porous Media
Keywords: nonlinear algorithms, finite-volume method, software tools, porous media, flows
(16 pages, 2006)

90. D. Niedziela, O. Iliev, A. Latz
On 3D Numerical Simulations of Viscoelastic Fluids

Keywords: non-Newtonian fluids, anisotropic viscosity, integral constitutive equation
(18 pages, 2006)

91. A. Winterfeld
Application of general semi-infinite Programming to Lapidary Cutting Problems
Keywords: large scale optimization, nonlinear programming, general semi-infinite optimization, design centering, clustering
(26 pages, 2006)

92. J. Orlik, A. Ostrovska
Space-Time Finite Element Approximation and Numerical Solution of Hereditary Linear Viscoelasticity Problems
Keywords: hereditary viscoelasticity; kern approximation by interpolation; space-time finite element approximation, stability and a priori estimate
(24 pages, 2006)

93. V. Rutka, A. Wiegmann, H. Andrä
EJIIM for Calculation of effective Elastic Moduli in 3D Linear Elasticity
Keywords: Elliptic PDE, linear elasticity, irregular domain, finite differences, fast solvers, effective elastic moduli
(24 pages, 2006)

94. A. Wiegmann, A. Zemitis
EJ-HEAT: A Fast Explicit Jump Harmonic Averaging Solver for the Effective Heat Conductivity of Composite Materials
Keywords: Stationary heat equation, effective thermal conductivity, explicit jump, discontinuous coefficients, virtual material design, microstructure simulation, EJ-HEAT
(21 pages, 2006)

95. A. Naumovich
On a finite volume discretization of the three-dimensional Biot poroelasticity system in multilayered domains
Keywords: Biot poroelasticity system, interface problems, finite volume discretization, finite difference method
(21 pages, 2006)

96. M. Krekel, J. Wenzel
A unified approach to Credit Default Swaption and Constant Maturity Credit Default Swap valuation
Keywords: LIBOR market model, credit risk, Credit Default Swaption, Constant Maturity Credit Default Swap-method
(43 pages, 2006)

97. A. Dreyer
Interval Methods for Analog Circiuts
Keywords: interval arithmetic, analog circuits, tolerance analysis, parametric linear systems, frequency response, symbolic analysis, CAD, computer algebra
(36 pages, 2006)

98. N. Weigel, S. Weihe, G. Bitsch, K. Dreßler
Usage of Simulation for Design and Optimization of Testing
Keywords: Vehicle test rigs, MBS, control, hydraulics, testing philosophy
(14 pages, 2006)

99. H. Lang, G. Bitsch, K. Dreßler, M. Speckert
Comparison of the solutions of the elastic and elastoplastic boundary value problems
Keywords: Elastic BVP, elastoplastic BVP, variational inequalities, rate-independency, hysteresis, linear kinematic hardening, stop- and play-operator
(21 pages, 2006)

100. M. Speckert, K. Dreßler, H. Mauch
MBS Simulation of a hexapod based suspension test rig
Keywords: Test rig, MBS simulation, suspension, hydraulics, controlling, design optimization
(12 pages, 2006)

101. S. Azizi Sultan, K.-H. Küfer
A dynamic algorithm for beam orientations in multicriteria IMRT planning
Keywords: radiotherapy planning, beam orientation optimization, dynamic approach, evolutionary algorithm, global optimization
(14 pages, 2006)

102. T. Götz, A. Klar, N. Marheineke, R. Wegener
A Stochastic Model for the Fiber Lay-down Process in the Nonwoven Production
Keywords: fiber dynamics, stochastic Hamiltonian system, stochastic averaging
(17 pages, 2006)

103. Ph. Süss, K.-H. Küfer
Balancing control and simplicity: a variable aggregation method in intensity modulated radiation therapy planning
Keywords: IMRT planning, variable aggregation, clustering methods
(22 pages, 2006)

104. A. Beaudry, G. Laporte, T. Melo, S. Nickel
Dynamic transportation of patients in hospitals
Keywords: in-house hospital transportation, dial-a-ride, dynamic mode, tabu search
(37 pages, 2006)

105. Th. Hanne
Applying multiobjective evolutionary algorithms in industrial projects
Keywords: multiobjective evolutionary algorithms, discrete optimization, continuous optimization, electronic circuit design, semi-infinite programming, scheduling
(18 pages, 2006)

106. J. Franke, S. Halim
Wild bootstrap tests for comparing signals and images
Keywords: wild bootstrap test, texture classification, textile quality control, defect detection, kernel estimate, nonparametric regression
(13 pages, 2007)

107. Z. Drezner, S. Nickel
Solving the ordered one-median problem in the plane
Keywords: planar location, global optimization, ordered median, big triangle small triangle method, bounds, numerical experiments
(21 pages, 2007)

108. Th. Götz, A. Klar, A. Unterreiter, R. Wegener
Numerical evidance for the non-existing of solutions of the equations desribing rotational fiber spinning
Keywords: rotational fiber spinning, viscous fibers, boundary value problem, existence of solutions
(11 pages, 2007)

109. Ph. Süss, K.-H. Küfer
Smooth intensity maps and the Bortfeld-Boyer sequencer
Keywords: probabilistic analysis, intensity modulated radiotherapy treatment (IMRT), IMRT plan application, step-and-shoot sequencing
(8 pages, 2007)

110. E. Ivanov, O. Gluchshenko, H. Andrä, A. Kudryavtsev
Parallel software tool for decomposing and meshing of 3d structures
Keywords: a-priori domain decomposition, unstructured grid, Delaunay mesh generation
(14 pages, 2007)

111. O. Iliev, R. Lazarov, J. Willems
Numerical study of two-grid preconditioners for 1d elliptic problems with highly oscillating discontinuous coefficients
Keywords: two-grid algorithm, oscillating coefficients, preconditioner
(20 pages, 2007)

112. L. Bonilla, T. Götz, A. Klar, N. Marheineke, R. Wegener
Hydrodynamic limit of the Fokker-Planck-equation describing fiber lay-down processes
Keywords: stochastic dierential equations, Fokker-Planck equation, asymptotic expansion, Ornstein-Uhlenbeck process
(17 pages, 2007)

113. S. Rief
Modeling and simulation of the pressing section of a paper machine
Keywords: paper machine, computational fluid dynamics, porous media
(41 pages, 2007)

114. R. Ciegis, O. Iliev, Z. Lakdawala
On parallel numerical algorithms for simulating industrial filtration problems
Keywords: Navier-Stokes-Brinkmann equations, finite volume discretization method, SIMPLE, parallel computing, data decomposition method
(24 pages, 2007)

115. N. Marheineke, R. Wegener
Dynamics of curved viscous fibers with surface tension
Keywords: Slender body theory, curved viscous bers with surface tension, free boundary value problem
(25 pages, 2007)

116. S. Feth, J. Franke, M. Speckert
Resampling-Methoden zur mse-Korrektur und Anwendungen in der Betriebsfestigkeit
Keywords: Weibull, Bootstrap, Maximum-Likelihood, Betriebsfestigkeit
(16 pages, 2007)

117. H. Knaf
Kernel Fisher discriminant functions – a concise and rigorous introduction
Keywords: wild bootstrap test, texture classification, textile quality control, defect detection, kernel estimate, nonparametric regression
(30 pages, 2007)

118. O. Iliev, I. Rybak
On numerical upscaling for flows in heterogeneous porous media
Keywords: numerical upscaling, heterogeneous porous media, single phase flow, Darcy's law, multiscale problem, effective permeability, multipoint flux approximation, anisotropy
(17 pages, 2007)

119. O. Iliev, I. Rybak
On approximation property of multipoint flux approximation method

Keywords: Multipoint flux approximation, finite volume method, elliptic equation, discontinuous tensor coefficients, anisotropy
(15 pages, 2007)

120. O. Iliev, I. Rybak, J. Willems
On upscaling heat conductivity for a class of industrial problems
Keywords: Multiscale problems, effective heat conductivity, numerical upscaling, domain decomposition
(21 pages, 2007)

121. R. Ewing, O. Iliev, R. Lazarov, I. Rybak
On two-level preconditioners for flow in porous media
Keywords: Multiscale problem, Darcy's law, single phase flow, anisotropic heterogeneous porous media, numerical upscaling, multigrid, domain decomposition, efficient preconditioner
(18 pages, 2007)

122. M. Brickenstein, A. Dreyer
POLYBORI: A Gröbner basis framework for Boolean polynomials
Keywords: Gröbner basis, formal verification, Boolean polynomials, algebraic cryptoanalysis, satisfiability
(23 pages, 2007)

123. O. Wirjadi
Survey of 3d image segmentation methods
Keywords: image processing, 3d, image segmentation, binarization
(20 pages, 2007)

124. S. Zeytun, A. Gupta
A Comparative Study of the Vasicek and the CIR Model of the Short Rate
Keywords: interest rates, Vasicek model, CIR-model, calibration, parameter estimation
(17 pages, 2007)

125. G. Hanselmann, A. Sarishvili
Heterogeneous redundancy in software quality prediction using a hybrid Bayesian approach
Keywords: reliability prediction, fault prediction, non-homogeneous poisson process, Bayesian model averaging
(17 pages, 2007)

126. V. Maag, M. Berger, A. Winterfeld, K.-H. Küfer
A novel non-linear approach to minimal area rectangular packing
Keywords: rectangular packing, non-overlapping constraints, non-linear optimization, regularization, relaxation
(18 pages, 2007)

127. M. Monz, K.-H. Küfer, T. Bortfeld, C. Thieke
Pareto navigation – systematic multi-criteria-based IMRT treatment plan determination
Keywords: convex, interactive multi-objective optimization, intensity modulated radiotherapy planning
(15 pages, 2007)

128. M. Krause, A. Scherrer
On the role of modeling parameters in IMRT plan optimization
Keywords: intensity-modulated radiotherapy (IMRT), inverse IMRT planning, convex optimization, sensitivity analysis, elasticity, modeling parameters, equivalent uniform dose (EUD)
(18 pages, 2007)

129. A. Wiegmann
Computation of the permeability of porous materials from their microstructure by FFF-Stokes
Keywords: permeability, numerical homogenization, fast Stokes solver
(24 pages, 2007)

130. T. Melo, S. Nickel, F. Saldanha da Gama
Facility Location and Supply Chain Management – A comprehensive review
Keywords: facility location, supply chain management, network design
(54 pages, 2007)

131. T. Hanne, T. Melo, S. Nickel
Bringing robustness to patient flow management through optimized patient transports in hospitals
Keywords: Dial-a-Ride problem, online problem, case study, tabu search, hospital logistics
(23 pages, 2007)

132. R. Ewing, O. Iliev, R. Lazarov, I. Rybak, J. Willems
An efficient approach for upscaling properties of composite materials with high contrast of coefficients
Keywords: effective heat conductivity, permeability of fractured porous media, numerical upscaling, fibrous insulation materials, metal foams
(16 pages, 2008)

133. S. Gelareh, S. Nickel
New approaches to hub location problems in public transport planning
Keywords: integer programming, hub location, transportation, decomposition, heuristic
(25 pages, 2008)

134. G. Thömmes, J. Becker, M. Junk, A. K. Vaikuntam, D. Kehrwald, A. Klar, K. Steiner, A. Wiegmann
A Lattice Boltzmann Method for immiscible multiphase flow simulations using the Level Set Method
Keywords: Lattice Boltzmann method, Level Set method, free surface, multiphase flow
(28 pages, 2008)

135. J. Orlik
Homogenization in elasto-plasticity
Keywords: multiscale structures, asymptotic homogenization, nonlinear energy
(40 pages, 2008)

136. J. Almquist, H. Schmidt, P. Lang, J. Deitmer, M. Jirstrand, D. Prätzel-Wolters, H. Becker
Determination of interaction between MCT1 and CAII via a mathematical and physiological approach
Keywords: mathematical modeling; model reduction; electrophysiology; pH-sensitive microelectrodes; proton antenna
(20 pages, 2008)

137. E. Savenkov, H. Andrä, O. Iliev
An analysis of one regularization approach for solution of pure Neumann problem
Keywords: pure Neumann problem, elasticity, regularization, finite element method, condition number
(27 pages, 2008)

138. O. Berman, J. Kalcsics, D. Krass, S. Nickel
The ordered gradual covering location problem on a network
Keywords: gradual covering, ordered median function, network location
(32 pages, 2008)

139. S. Gelareh, S. Nickel
Multi-period public transport design: A novel model and solution approaches
Keywords: Integer programming, hub location, public transport, multi-period planning, heuristics
(31 pages, 2008)

140. T. Melo, S. Nickel, F. Saldanha-da-Gama
Network design decisions in supply chain planning
Keywords: supply chain design, integer programming models, location models, heuristics
(20 pages, 2008)

141. C. Lautensack, A. Särkkä, J. Freitag, K. Schladitz
Anisotropy analysis of pressed point processes
Keywords: estimation of compression, isotropy test, nearest neighbour distance, orientation analysis, polar ice, Ripley's K function
(35 pages, 2008)

142. O. Iliev, R. Lazarov, J. Willems
A Graph-Laplacian approach for calculating the effective thermal conductivity of complicated fiber geometries
Keywords: graph laplacian, effective heat conductivity, numerical upscaling, fibrous materials
(14 pages, 2008)

143. J. Linn, T. Stephan, J. Carlsson, R. Bohlin
Fast simulation of quasistatic rod deformations for VR applications
Keywords: quasistatic deformations, geometrically exact rod models, variational formulation, energy minimization, finite differences, nonlinear conjugate gradients
(7 pages, 2008)

144. J. Linn, T. Stephan
Simulation of quasistatic deformations using discrete rod models
Keywords: quasistatic deformations, geometrically exact rod models, variational formulation, energy minimization, finite differences, nonlinear conjugate gradients
(9 pages, 2008)

145. J. Marburger, N. Marheineke, R. Pinnau
Adjoint based optimal control using mesh-less discretizations
Keywords: Mesh-less methods, particle methods, Eulerian-Lagrangian formulation, optimization strategies, adjoint method, hyperbolic equations
(14 pages, 2008

146. S. Desmettre, J. Gould, A. Szimayer
Own-company stockholding and work effort preferences of an unconstrained executive
Keywords: optimal portfolio choice, executive compensation
(33 pages, 2008)

147. M. Berger, M. schröder, K.-H. Küfer
A constraint programming approach for the two-dimensional rectangular packing problem with orthogonal orientations
Keywords: rectangular packing, orthogonal orientations non-overlapping constraints, constraint propagation
(13 pages, 2008)

148. K. Schladitz, C. Redenbach, T. Sych, M. Godehardt

Microstructural characterisation of open foams using 3d images

Keywords: virtual material design, image analysis, open foams
(30 pages, 2008)

149. E. Fernández, J. Kalcsics, S. Nickel, R. Ríos-Mercado

A novel territory design model arising in the implementation of the WEEE-Directive

Keywords: heuristics, optimization, logistics, recycling
(28 pages, 2008)

150. H. Lang, J. Linn

Lagrangian field theory in space-time for geometrically exact Cosserat rods

Keywords: Cosserat rods, geometrically exact rods, small strain, large deformation, deformable bodies, Lagrangian field theory, variational calculus
(19 pages, 2009)

151. K. Dreßler, M. Speckert, R. Müller, Ch. Weber

Customer loads correlation in truck engineering

Keywords: Customer distribution, safety critical components, quantile estimation, Monte-Carlo methods
(11 pages, 2009)

152. H. Lang, K. Dreßler

An improved multiaxial stress-strain correction model for elastic FE postprocessing

Keywords: Jiang's model of elastoplasticity, stress-strain correction, parameter identification, automatic differentiation, least-squares optimization, Coleman-Li algorithm
(6 pages, 2009)

153. J. Kalcsics, S. Nickel, M. Schröder

A generic geometric approach to territory design and districting

Keywords: Territory design, districting, combinatorial optimization, heuristics, computational geometry
(32 pages, 2009)

154. Th. Fütterer, A. Klar, R. Wegener

An energy conserving numerical scheme for the dynamics of hyperelastic rods

Keywords: Cosserat rod, hyperealstic, energy conservation, finite differences
(16 pages, 2009)

155. A. Wiegmann, L. Cheng, E. Glatt, O. Iliev, S. Rief

Design of pleated filters by computer simulations

Keywords: Solid-gas separation, solid-liquid separation, pleated filter, design, simulation
(21 pages, 2009)

156. A. Klar, N. Marheineke, R. Wegener

Hierarchy of mathematical models for production processes of technical textiles

Keywords: Fiber-fluid interaction, slender-body theory, turbulence modeling, model reduction, stochastic differential equations, Fokker-Planck equation, asymptotic expansions, parameter identification
(21 pages, 2009)

157. E. Glatt, S. Rief, A. Wiegmann, M. Knefel, E. Wegenke

Structure and pressure drop of real and virtual metal wire meshes

Keywords: metal wire mesh, structure simulation, model calibration, CFD simulation, pressure loss
(7 pages, 2009)

158. S. Kruse, M. Müller

Pricing American call options under the assumption of stochastic dividends – An application of the Korn-Rogers model

Keywords: option pricing, American options, dividends, dividend discount model, Black-Scholes model
(22 pages, 2009)

159. H. Lang, J. Linn, M. Arnold

Multibody dynamics simulation of geometrically exact Cosserat rods

Keywords: flexible multibody dynamics, large deformations, finite rotations, constrained mechanical systems, structural dynamics
(20 pages, 2009)

160. P. Jung, S. Leyendecker, J. Linn, M. Ortiz

Discrete Lagrangian mechanics and geometrically exact Cosserat rods

Keywords: special Cosserat rods, Lagrangian mechanics, Noether's theorem, discrete mechanics, frame-indifference, holonomic constraints
(14 pages, 2009)

161. M. Burger, K. Dreßler, A. Marquardt, M. Speckert

Calculating invariant loads for system simulation in vehicle engineering

Keywords: iterative learning control, optimal control theory, differential algebraic equations(DAEs)
(18 pages, 2009)

162. M. Speckert, N. Ruf, K. Dreßler

Undesired drift of multibody models excited by measured accelerations or forces

Keywords: multibody simulation, full vehicle model, force-based simulation, drift due to noise
(19 pages, 2009)

Status quo: May 2009